Three-dimensional scaffolds for tissue engineering applications : role of porosity and pore size

Loh, Qiu Li; Choong, Cleo Swee Neo

2013

Loh, Q. L., & Choong, C. (2013). Three-dimensional scaffolds for tissue engineering applications : role of porosity and pore size. Tissue engineering Part B: reviews, 19(6), 485-502.

https://hdl.handle.net/10356/106120

https://doi.org/10.1089/ten.teb.2012.0437

TISSUE ENGINEERING: Part B
Volume 19, Number 6 2013

DOI: 10.1089/ten.teb.2012.0437

Three-Dimensional Scaffolds for Tissue Engineering Applications: Role of Porosity and Pore Size

Qiu Li Loh, BEng, and Cleo Choong, DPhil (Oxon), MBA, MEng (Hons), CEng MIMMM

Tissue engineering applications commonly encompass the use of three-dimensional (3D) scaffolds to provide a suitable microenvironment for the incorporation of cells or growth factors to regenerate damaged tissues or organs. These scaffolds serve to mimic the actual *in vivo* microenvironment where cells interact and behave according to the mechanical cues obtained from the surrounding 3D environment. Hence, the material properties of the scaffolds are vital in determining cellular response and fate. These 3D scaffolds are generally highly porous with interconnected pore networks to facilitate nutrient and oxygen diffusion and waste removal. This review focuses on the various fabrication techniques (e.g., conventional and rapid prototyping methods) that have been employed to fabricate 3D scaffolds of different pore sizes and porosity. The different pore size and porosity measurement methods will also be discussed. Scaffolds with graded porosity have also been studied for their ability to better represent the actual *in vivo* situation where cells are exposed to layers of different tissues with varying properties. In addition, the ability of pore size and porosity of scaffolds to direct cellular responses and alter the mechanical properties of scaffolds will be reviewed, followed by a look at nature's own scaffold, the extracellular matrix. Overall, the limitations of current scaffold fabrication approaches for tissue engineering applications and some novel and promising alternatives will be highlighted.

Introduction

Three-dimensional (3D) scaffolds are commonly used for drug delivery,[1,2] investigation of cell behavior and material studies in the field of tissue engineering.[3–5] Three-dimensional scaffolds are typically porous, biocompatible and biodegradable materials that serve to provide suitable microenvironments, that is, mechanical support, physical, and biochemical stimuli for optimal cell growth and function (Fig. 1).[6–9] The porosity and pore size of 3D scaffolds have direct implications on their functionality during biomedical applications. Open porous and interconnected networks are essential for cell nutrition, proliferation, and migration for tissue vascularization and formation of new tissues (Fig. 2).[6,7,10] A porous surface also serves to facilitate mechanical interlocking between the scaffolds and surrounding tissue to improve the mechanical stability of the implant.[11] In addition, the network structure of the pores assists in guiding and promoting new tissue formation.[9,12] Materials with high porosity enable effective release of biofactors such as proteins, genes, or cells and provide good substrates for nutrient exchange. However, the mechanical property that is important in maintaining the structural stability of the biomaterial is often compromised as the result of increased porosity.[7] Hence, a balance between the mechanical and mass transport function of the scaffolds should exist for an optimal scaffold system. As a result, the final porosity and pore sizes of the scaffold should be taken into account in accordance to the intended eventual application during scaffold design and fabrication stages. This review is focused on the fabrication of porous 3D scaffolds, the methods for evaluating porosity and pore sizes of 3D constructs, and some of the reported effects of pore size and porosity on cell behavior and overall mechanical properties. A more general overview of the various scaffold fabrication and porosity measurement techniques has been covered in previous reviews.[11,13–15]

Fabrication of 3D Porous Scaffolds

Various techniques have been used for the fabrication of 3D scaffolds. Generally, conventional fabrication techniques such as salt leaching, gas forming, phase separation, and freeze-drying (Fig. 3) do not enable precise control of internal scaffold architecture or the fabrication of complex architectures that could be achieved by rapid prototyping techniques (Fig. 4) using computer-aided design (CAD) modeling.[8] These conventional techniques also require good fabrication skills to maintain consistency in scaffold architecture.

Division of Materials Technology, School of Materials Science and Engineering, Nanyang Technological University, Singapore, Singapore.

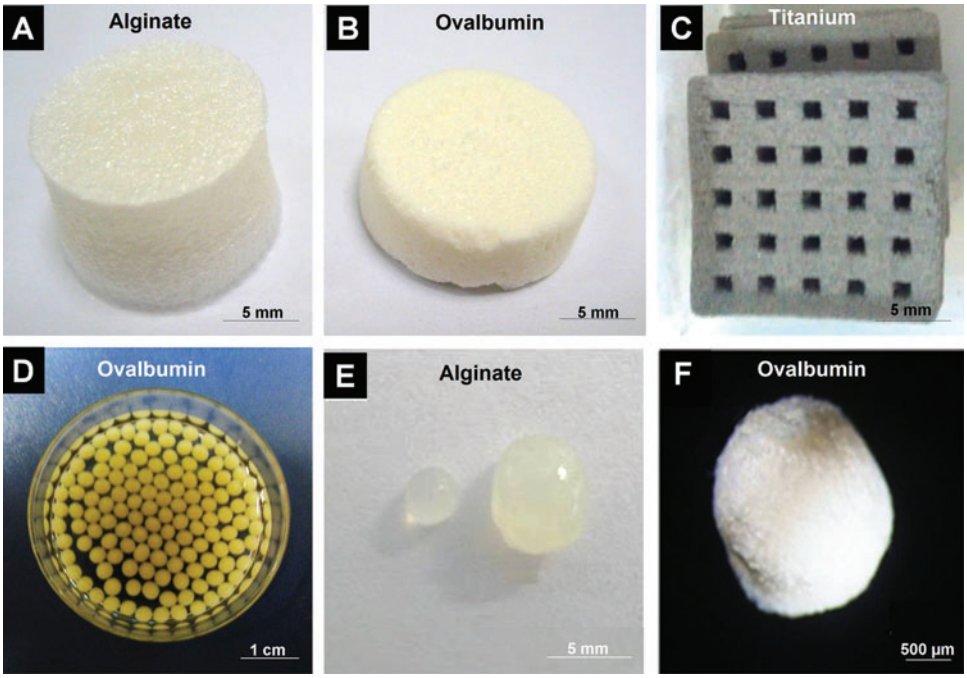

FIG. 1. Images of three-dimensional (3D) **(A–C)** scaffolds, **(D, E)** hydrogels, and **(F)** microcarriers of various geometry, size and morphology used in tissue engineering applications. Color images available online at www.liebertpub.com/teb

Another limitation present is the use of toxic solvents, which may result in cell death if they are not completely removed.[16] Besides, scaffolds fabricated using these traditional processing techniques have compressive moduli at a maximum of 0.4 MPa, which is much lower than hard tissue (10–1500 MPa) or most soft tissues (0.4–350 MPa).[7,17] Hence, the development of rapid prototyping fabrication techniques enables the fabrication of scaffolds with improved mechanical properties, with moduli ranging from soft to hard tissues.[18,19] Conversely, rapid prototyping techniques have better design repeatability, part consistency, and control of scaffolds architecture at both micro and macro levels.[16,20,21] Although rapid prototyping techniques may have several advantages, some limitations and challenges still remain

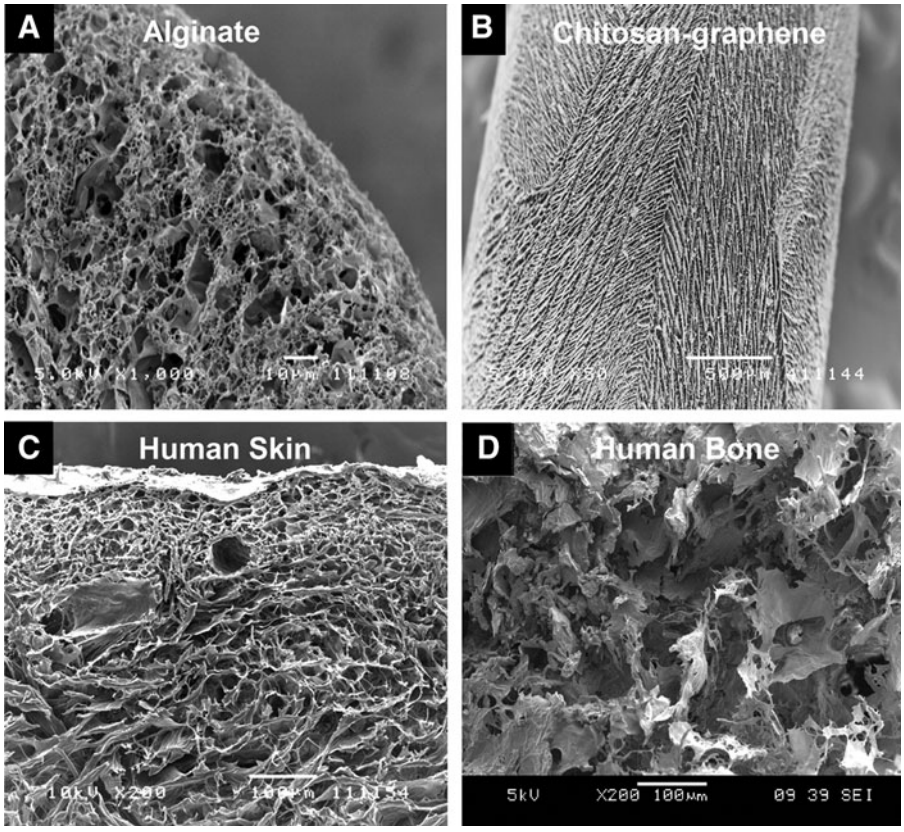

FIG. 2. Scanning electron microscopy (SEM) images of **(A, B)** porous scaffolds and **(C, D)** human tissues with interconnected pores. Tissue engineered scaffolds should ideally mimic the porosity, pore size, and function of native human tissues.

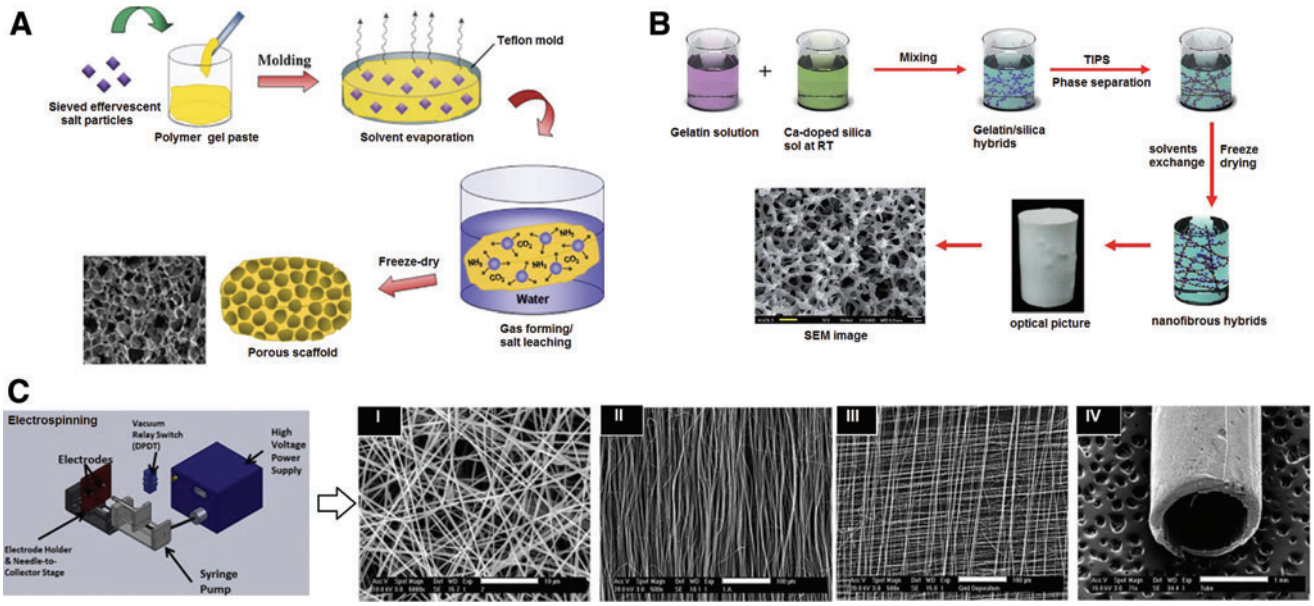

FIG. 3. Schematic illustrations of some conventional fabrication methods: **(A)** gas foaming/particulate leaching, **(B)** thermally induced phase separation, and **(C)** electrospinning used to obtain porous scaffolds. Images adapted and reproduced by permission of Elsevier and The Royal Society of Chemistry (http://dx.doi.org/10.1039/C2JM31290E).[27–29] Color images available online at www.liebertpub.com/teb

such as the limited number of biomaterials that can be processed by rapid prototyping compared to conventional techniques.[22] Other approaches that mimic the way that tissues are formed in the body, and their nanofibrous structure can be found in modular assembly methods, and electrospinning methods.[23–26]Alternative approaches to prefabrication of scaffolds prior to cell seeding include cell encapsulation, and the development of tunable scaffolds that have the potential for further modification postimplantation. The advantages and disadvantages of these alternative approaches will also be discussed in this section.

Salt leaching

This method has been commonly used to fabricate scaffolds for tissue engineering applications.[14,36,37] Using this

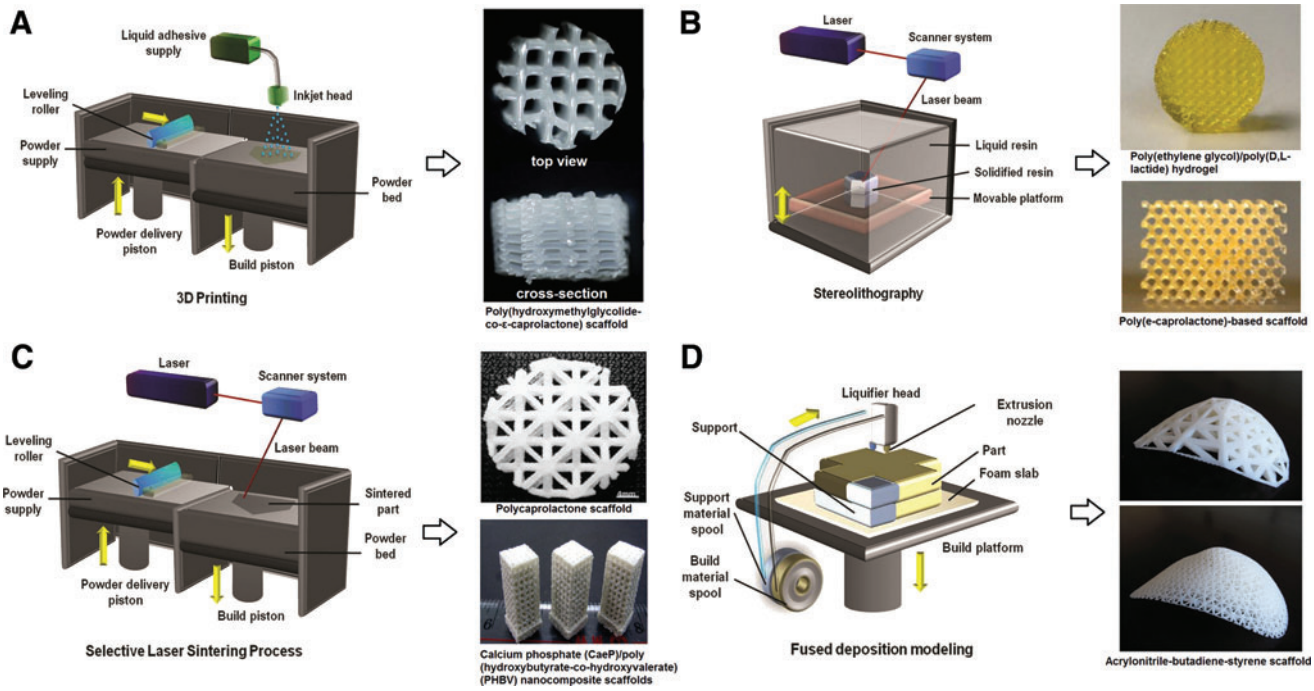

FIG. 4. Schematic illustrations and images of 3D scaffolds fabricated from rapid prototyping methods: **(A)** 3D printing, **(B)** selective laser sintering, **(C)** stereolithography, and **(D)** fused deposition modeling. Images adapted and reproduced by permission of Elsevier.[30–35] Color images available online at www.liebertpub.com/teb

method, porogen or salt crystals (e.g., sodium chloride) are placed into a mold and a polymer is then added to fill in the remaining spaces. The polymer is subsequently hardened and the salt is removed via dissolution in a solvent such as water or alcohol. A hardened polymer with pores will be formed once all the salt leaches out.[38] The pore size of the scaffolds can be controlled by the size of porogen used. The porosity and pore size of the scaffold can also be controlled by varying the amount and size of the salt particles respectively.[14] The main advantage of this technique is the use of small amounts of polymer, which minimizes any polymer wastage unlike those methods that require large machinery and produces unused material parts during fabrication such as some of the rapid prototyping techniques. However, the interpore openings and pore shape of scaffolds produced by this method is not controllable.[14] Thus, by combining salt leaching with other scaffold fabrication techniques, it may be possible to create scaffolds with better pore interconnectivity and structure.[39]

Gas forming

In this technique, gas is used as a porogen.[40] Solid discs of polymers such as polyglycolide and poly-L-lactide are first formed by compression molding at high temperatures prior to the application of high-pressure carbon dioxide gas through the discs for a few days before reducing the pressure back to atmospheric level.[41] The main advantage of using this method is the elimination of the use of harsh chemical solvents, thus removing the leaching step from the fabrication process, which subsequently reduces the overall fabrication time. However, it is difficult to ensure pore connectivity and control of the pore sizes by gas forming.[42,43] Further, the application of high temperatures during disc formation also prohibits the use of bioactive molecules in the scaffolds.[44] With this gas forming technique, scaffolds with porosity up to 93% and pore sizes up to 100 μm can be fabricated.[44]

Phase separation

In general, a polymer is first dissolved in a suitable solvent and subsequently placed in a mold that will be rapidly cooled until the solvent freezes. The solvent is then removed by freeze-drying and pores will be left behind in the polymer. This method also does not necessitate an extra leaching step, but the addition of organic solvents such as ethanol or methanol inhibits the incorporation of bioactive molecules or cells during scaffold fabrication. In addition, the small pore sizes obtained is another limiting factor of scaffolds fabricated by phase separation.[14,44] Different types of phase separation techniques available include thermally-induced, solid-liquid, and liquid–liquid phase separation.[45–47]

Freeze-drying

When materials are freeze-dried, the frozen water is sublimated directly into the gas phase, which results in pore formation.[48] This method was first used by Whang *et al.* to fabricate PLGA scaffolds.[49] The porosity and pore sizes of the scaffolds fabricated are largely dependent on the parameters such as ratio of water to polymer solution and viscosity of the emulsion.[44] The pore structure of the scaffolds can be controlled by varying the freezing temperature.[50] The advantages of this process are the elimination of several rinsing steps since dispersed water and polymer solvents can be removed directly.[49] Moreover, polymer solutions can be used directly, instead of the need to cross-link any monomers. However, the freeze-drying process should be controlled to reduce heterogeneous freezing to increase scaffold homogeneity.[50]

3D printing

Three-dimensional printing involves the laying down of successive layers of material to form 3D models, thus enabling better control of pore sizes, pore morphology, and porosity of matrix as compared with other fabrication methods.[7,51] In general, the binder solution is added onto the powder bed from an "inkjet" print head. A 2D layer will be printed and a new layer of powder will be laid down subsequently. The process repeats and the layers will merge when fresh binder solution is deposited each time. The finished component will be removed and any unbound powder will be left behind. This technique allows more complex 3D shapes with high resolution and controlled internal structures to be fabricated.[52] There are two types of pores fabricated by this process, that is, pore by design and pore by process. However, only a limited number of polymers can be fabricated using this method given the high temperatures involved in this method. In addition, ceramic scaffolds obtained by this method have better mechanical strengths, but require a second sintering process at high temperatures to improve on the brittle toughness. Moreover, preprocessing of base biomaterials is necessary as they are usually not in powdered form.[53,54]

Selective laser sintering

In the selective laser sintering (SLS) process, regions on the powder bed are fused layer by layer using a computer controlled laser beam to form a 3D solid mass.[55–57] Due to the stepwise addition of materials, SLS enables the construction of scaffolds with complex geometries. Moreover, any powdered biomaterial that will fuse but not decompose under a laser beam can be used in this fabrication process. SLS is fast, cost effective and does not require the use of any organic solvents.[58] However, the elevated temperatures needed require high local energy input. In addition, degradation of the material, for example, chain scission, cross-linking, and oxidation processes may occur due to exposure to the laser beam.[59]

Stereolithography

This is one of the earliest rapid prototyping techniques and it involves the use of ultraviolet laser to polymerize liquid ultraviolet curable photopolymer resin layer-by-layer, which then solidifies to form a 3D model.[60] The excess resin will be drained after the complete model is raised out of the vat for curing in an oven. This rapid prototyping technique allows quick fabrication of materials with a wide variety of shapes. The resolution of each layer is dependent on the resolution of the elevator layer and the spot size of the laser.[61] However, due to the application of additional curing step to improve the model's property, the final resolution is

compromised of shrinkage that typically occurs in this postprocessing step.[62,63] Also, there is a limited variety of photopolymerisable materials that are suitable for biomedical applications.

Fused deposition modeling

In fused deposition modeling, a small temperature controlled extruder is used to allow thermoplastic material to be deposited onto a platform in a layer by layer manner to form a 3D material.[64–66] The base platform will be lowered at the end of each layer so that subsequent layers can then be added onto them. Like the other rapid prototyping methods, fused deposition modeling makes use of computer generated solid or surface models to enable precise deposition of thin layers of the semi-molten polymer. However, the disadvantage of this method is the use of elevated temperatures, which limits the type of biomaterials that can be used.

Electrospinning

During solution electrospinning, a voltage is applied to generate a potential difference between a polymeric solution and a collecting target.[67,68] A polymeric jet of fluid will be ejected from a spinneret or tip of a capillary when the surface tension of the fluid is overcomed by the electrical charges. The macromolecular entanglements present in the polymeric solution will cause the fluid jet to be drawn toward the collector as it does not go through Rayleigh instabilities, that is, formation of droplets due to breaking up of the fluid jet.[67] As the fluid jet approaches the collector, twisting occurs due to the presence of higher surface charge density. Ultimately, a mesh of electrospun fibers will be collected. The diameter of each fiber can be controlled by altering the concentration and flow rate of the polymer solution, and varying the distance between the needle and collector.[68,69] Pham *et al.* showed that the average pore size of electrospun scaffolds increased with increasing fiber diameter.[70] Some advantages of electrospun scaffolds include the presence of high surface area for cell attachment and high porosity to facilitate nutrient and waste exchange.[71–73] Solution electrospinning is also a simple and inexpensive scaffold fabrication technique, and a wide range of polymeric solutions can be used to fabricate the scaffolds. However, the main disadvantage of electrospinning is the involvement of toxic organic solvents during fabrication, which can be harmful to cells.[74] Thus, melt electrospinning, which does not involve the use of organic solvents, is an alternative to solution electrospinning.[75,76] In melt electrospinning, the polymer is heated with an electric heater or CO_2 laser above its melting or glass transition temperature.[77,78] However, as polymer melts have lower charge density and are more viscous than its solution, fibers obtained from melt electrospinning process are thicker than those fabricated from solution electrospinning.[75,79]

Cell encapsulation

Instead of prefabricating porous scaffolds and culturing cells on them subsequently, an alternative is to incorporate cells during the scaffold fabrication process. Cell encapsulation, involving entrapping cells inside a material, has been commonly used to protect cells from the immune system.[80] Generally, cells are mixed with the encapsulation material before gelation occurs. Hence, the encapsulation material and gelation process need to be cytocompatible.[81] Reviews by Hunt & Grover and Nicodemus & Bryant discussed some of the materials commonly used for cell encapsulation.[82,83] Using this method, cells can either be individually encapsulated or a fixed number of cells can be enclosed in a certain volume of material, in spherical or fiber forms.[84–86] Currently, the main limitation of cell encapsulation is the balance between appropriate diffusion coefficient for the transport of oxygen and nutrients to the cells and to the retention of immunoprotective properties.[87] However, it has been shown by our group and others that processing conditions, the use of a coating layer, can play a role in modifying the porosity or permeability of the encapsulation material.[88–90] Others have used superporous hydrogels (SPHs) instead of nonporous hydrogels (NPHs) as their encapsulation material to facilitate more favorable diffusion properties.[42] SPHs have an internal pore architecture that allow cell attachment and proliferation following cell seeding. Conversely, if cells were seeded onto the NPHs, they will only attach onto the surface due to the absence of an internal pore architecture. For cell encapsulation, cells will generally spread throughout the NPHs, but will only be present inside the interpore connections for SPHs (Fig. 5). Using superporous poly(ethylene glycol) diacrylate (PEGDA) hydrogel scaffolds, NIH-3T3 fibroblast cells were encapsulated into superporous PEGDA hydrogels, instead of seeding cells directly onto prefabricated

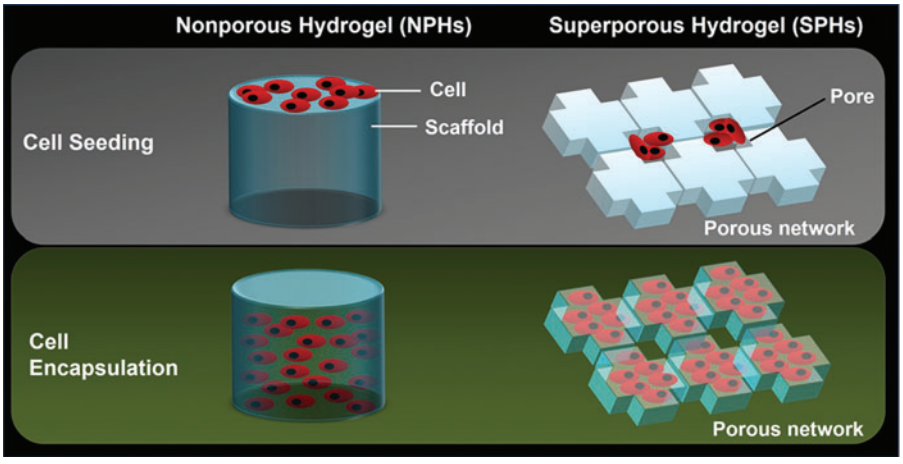

FIG. 5. Schematic illustration of cell culture for nonporous hydrogels (NPHs) and superporous hydrogels (SPHs). Cell seeding onto NPHs will result in cells proliferating on the surface, while cell encapsulation entraps cells within the scaffold. For SPHs, cells will proliferate between the pores when they are seeded onto the scaffolds, or entrapped in the interior during the encapsulation process. Color images available online at www.liebertpub.com/teb

SPH scaffolds.[42] These fibroblasts were also encapsulated in NPHs and it was observed that the decrease in number of viable cells was two-folds higher than in SPHs. The main advantages of cell encapsulation are the ability to provide immunoshielding for cells and the possibility of fabricating injectable forms.

Porosity and Pore Size Measurement Techniques

Various equipment and computer software can be used to measure porosity and pore size of scaffolds. The total porosity is related to the amount of pore space present in the scaffolds. Physical properties such as material or bulk density of the scaffolds can be used to calculate the total porosity. Fluid intrusion methods can also be indirectly used to measure the porosity of scaffolds. Besides using these physical characterization methods, imaging techniques can also be employed for porosity measurements.

Gravimetric method

The total porosity (Π) of scaffolds can be determined by gravimetric method using the bulk and true density of the material as shown in Eq. 1 and 2 below.[81,91–93]

$$\rho_{\text{scaffold}} = \frac{mass}{volume} \quad (1)$$

$$Total\ porosity\ (\Pi) = 1 - \frac{\rho_{\text{scaffold}}}{\rho_{\text{material}}} \quad (2)$$

where ρ_{scaffold} = apparent density of the scaffold and ρ_{material} = density of the material.

The volume is calculated by measuring the length, width, and height of the sample. Although this is a simple and fast method, it is a rough estimation of the actual porosity as significant errors can be made while determining the actual volume of the scaffold.[93] However, this method is preferred for materials that cannot withstand the high pressures used in other porosity determination methods, for example, layers of nanofiber mats.[94]

Mercury porosimetry

This method allows the determination of the total pore volume fraction, the average pore diameter, and pore size distribution of 3D materials.[93,95,96] Scaffolds are placed in a mercury penetrometer and subsequently infused with mercury under increasing pressures, up to a maximum of 414 MPa (Fig. 6A).[11] The mercury is forced into the pores of the scaffolds under high pressures. Since mercury is non-wetting, it only fills the pores when the applied pressure is greater than the tension forces of the surface meniscus. Thus pores that are smaller will have higher tension forces due to greater curvature of surface meniscus and they require higher pressure to fill the pore volume with mercury. This technique has been used to analyze the pore characteristics of various scaffold types, for example, hydroxyapatite scaffolds, poly (α-hydroxy acid) foam scaffold, and electrospun poly (ε-caprolactone) nano- or micro-fiber scaffolds.[70,81,97–100] Although mercury intrusion is more reliable than others that require manual measurements that might vary based on individuals, it has several drawbacks relating to the high pressures involved. Hence, it should be noted that lower pressures should be used for biomaterials that compress or collapse easily, for example, hydrogels.[101] Moreover, materials with thin cross sections may also be destroyed if they are analyzed at high pressures.[94] Another disadvantage is the toxicity and cost of mercury.

Liquid displacement method

The porosity of scaffolds can also be measured using a displacement liquid that is a not a solvent of the polymers, for example, ethanol, and is capable of penetrating into the pores easily but do not cause size shrinkage or swelling to the material being tested.[102] In brief, the scaffold will be placed in a cylinder with a known volume of the displacement liquid and a series of evacuation–repressurization cycles will be done to force the liquid into the pores (Fig. 6B).[103] This is also another simple technique that can be carried out easily, but is an indirect way of measuring porosity.

The open porosity can be calculated using the following method (Eq. 3).[104–106]

$$Porosity = \frac{V_1 - V_3}{V_2 - V_3} \quad (3)$$

where V_1 = known volume of liquid that is used to submerge the scaffold (but not a solvent for the scaffold), V_2 = volume of the liquid and liquid-impregnated scaffold, and V_3 = remaining liquid volume when the liquid-impregnated scaffold is removed.

Scanning electron microscopy analysis

Various computer software such as SemAfore or ImageJ can be used to analyze scanning electron microscopy (SEM) images to measure pore sizes (Fig. 6C) and porosity.[107–111] From the SEM images, an estimation of the cross-sectional area, interconnectivity, and wall thickness can also be obtained.[112] However, to obtain accurate measurements, sectioning should be done carefully so as to avoid compression of the scaffold cross section. ImageJ is an image processing program that can be used for various purposes with user-written plugins, for example, 3D live-cell imaging or radiological image processing. For porosity measurements, ImageJ with jPOR macro has been recently established and used to quantify the total optical porosity of blue-stained thin sections.[113] This technique allows rapid measurement of porosity from thin section images. It is easy to use and does not require specialist training.

Microcomputed tomography imaging

Microcomputed tomography (Micro-CT) imaging can be used to provide precise information on the 3D morphology of scaffolds (Fig. 6D). During the imaging process, X-rays are used to divide the scaffold into a series of 2D thin sections. The emerging X-rays will be captured by a detector array that calculates the X-ray path and attenuation coefficients.[112] The attenuation coefficient will be correlated to the material density to obtain a 2D map that shows the various material phases within the scaffold. Intricate details can be imaged at high resolutions, but longer time and more data storage space is required. Subsequently, 3D modeling programs, for example, Velocity, Anatomics, and Mimics are used to create 3D models from the individual 2D maps obtained earlier. Image thresholding should also be executed before 3D

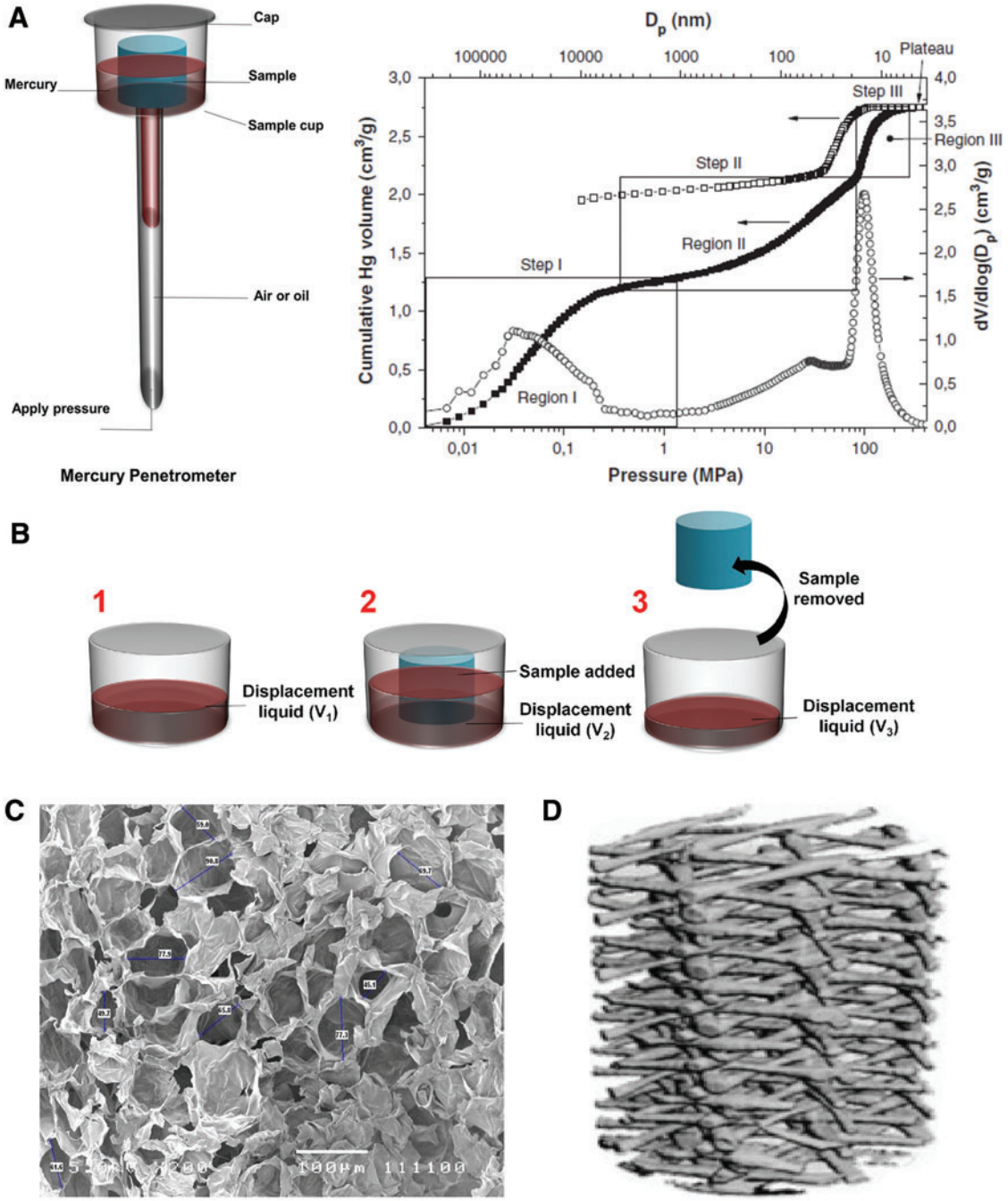

FIG. 6. Schematic illustration of **(A)** mercury porosimetry, **(B)** three-step liquid displacement process, **(C)** SEM imaging technique, and **(D)** microcomputed tomography imaging used for porosity or pore size measurement of scaffolds. Images adapted and reproduced by permission of Elsevier and IOP Publishing Ltd. (DOI: 10.1088/1758-5082/3/3/034114).[121,122] Color images available online at www.liebertpub.com/teb

modeling, which would otherwise affect subsequent analysis. This method is noninvasive and does not require any physical sectioning, which enables the scaffold to be reused for other analysis after scanning.[11] Moreover, it also eliminates the use of any toxic chemicals.[112] Micro-CT is also suitable for scaffolds with intricate interior structures. However, this technique is not suitable for scaffolds that contains metals since X-rays will be heavily attenuated by them, which results in bright and dark grainy scan images that causes loss of important details.[112]

CAD models

CAD models can be used to design 3D scaffolds of designated structure, pore size, and porosity.[114] It is one of the commonly used technologies in the aspect of Computer-Aided Tissue Engineering, where 3D visualization and simulation are enabled for the manufacturing of 3D complex tissue models.[115] Rapid prototyping techniques such as 3D printing, stereolithography, and fused deposition modeling utilizes CAD models to reproducibly fabricate very precise

structures or biological tissue replicas.[61] For CAD models, porosity is calculated from Eq. 4.[116]

$$Porosity = 1 - \frac{V_{solid}}{V_{total}} \times 100\% \quad (4)$$

where V_{solid} = volume of solid and V_{total} = total volume of scaffold.

Permeability-based method

Scaffold permeability has been used to determine the pore size and fiber diameter of electrospun fibrinogen scaffolds.[117] Using this method, Carr *et al.* used a flowmeter to pass a fluid through an electrospun scaffold to calculate the scaffold's pore properties.[118,119] The amount of fluid that passes through the scaffold area over time is determined. Using this flowmeter designed by Sell *et al.*, the permeability (T) was calculated using the equations shown in Eq. 5 and 6.[117–119]

$$p = \rho g h \quad (5)$$

$$T = \frac{Q\eta h_s}{Ftp} \quad (6)$$

where p = applied head pressure (Pa), ρ = density of water, g = gravitational force, h = total height of the system (1.5 m), Q = volume of fluid that passed through the scaffold over a period of time (t), η = viscosity of the fluid, h_s = thickness of scaffold, and F = cross-sectional area of the scaffold perpendicular to fluid flow.

After obtaining the scaffold permeability values, the pore radius (r) of the scaffold can be calculated according to Eq. 7.

$$r = \frac{0.5093}{T^{-\frac{1}{2}}} \quad (7)$$

Capillary flow porometry

This is a nondestructive method that can be used to measure the pore size and distribution of scaffolds. In this technique, a nonreacting gas is used to flow through the scaffold.[120] This method can be used on either a dry scaffold or a wet scaffold that is hydrated using a liquid with known surface tension. The change in flow rate is then calculated using the difference in pressure for the dry and wet processes. This technique utilizes low pressure during the process, thus it is suitable for measuring the porous structure of nanofiber membranes. The pore size (D) can be calculated with a software (Porous Media, Inc.) using Eq. 8.

$$D = \frac{4Y\cos\theta}{\Delta p} \quad (8)$$

where Y = surface tension of liquid, θ = contact angle of liquid, and Δp = difference in pressure.

Gradient Porosity

Tissue engineering scaffolds should ideally exhibit similar structural complexity as the native tissue to satisfy the intended biological function. Natural porous materials, including tissues, typically have a gradient porous structure (GPS), in which porosity is not uniform. Rather, it is distributed in such a manner so as to maximize the overall performance of the structure.[123] Gradient porosity is observed in bone tissues and this optimizes the material's response to external loading.[15] Gradient porosity is also observed in tissues such as the skin, where the pore size increases with distance away from the skin surface. Gradient porosity also enables specific cell migration during tissue regeneration, and is also required for the treatment of articular cartilage defects in osteochondral tissue engineering. In general, macropores are essential to provide space for vascularization and tissue ingrowth, since gas diffusion, nutrient supply, and waste removal is facilitated. However, a denser structure will improve the mechanical properties of scaffolds and enable better cell attachment and intracellular signaling.[124,125] Gradient porosity also enables specific cell migration during tissue regeneration, and is also required for the treatment of articular cartilage defects in osteochondral tissue engineering.[125,126] Hence, a fine balance between adequate porosity and mechanical stability is required. This will be discussed in more detail in the "Mechanical property" section of this review.

As a potential application in bone tissue engineering, 45S5 Bioglass®-derived glass–ceramic scaffolds with graded pore sizes and different shapes have been produced by foam replication technique, where preformed polyurethane (PU) foams have been used as sacrificial templates.[125] These PU foam templates with tailored gradient porosity were compressed using aluminium molds. Hydroxyapatite/tricalcium phosphate (HA/TCP) ceramic scaffolds with gradient porosity were also fabricated using a room temperature camphene-based freeze-casting method as a potential bone graft substitute.[127] Calcium phosphate-based ceramics, for example, HA have excellent biocompatibility, bioactivity, and osteoconductivity, thus enabling them to be suitable materials for bone tissue engineering applications. Freeze casting allows the fabrication of graded scaffolds with better mechanical properties than foam replication techniques as the latter generally generates defects during the pyrolysis of the polymer foam template, which results in scaffolds with poorer mechanical properties.[128] In the freeze casting process, ceramic slurry that is usually aqueous based, is frozen in a mould at low temperatures, then demoulded, and subsequently sublimated for vehicle removal so as to obtain a green body.[129] This freeze casting method showed potential in generating defect-free scaffolds with controlled porosity and pore sizes, and having appropriate compressive properties for tissue engineering applications.[127]

Cylindrical polycaprolactone (PCL) scaffolds with gradually increasing pore sizes along the longitudinal direction were also successfully fabricated using a novel centrifugation method developed by Oh *et al.*[130] These scaffolds with pore size gradient were formed by adding fibril-like PCL into a cylindrical mold that was subjected to centrifugation and subsequently heat-treated to enable fibril bonding. The gradual increment of the centrifugal force along the cylindrical axis causes the formation of a pore size gradient. The centrifugal speed can also be adjusted to control the pore size range of the scaffolds. These scaffolds with gradient pore sizes are good tools that can be used for the systemic study of cellular or tissue interaction with scaffolds.

Effect of Porosity and Pore Size on Cell Behavior and Mechanical Property

Cell proliferation and differentiation

Cell behavior is directly affected by the scaffold architecture since the extracellular matrix (ECM) provides cues that influence the specific integrin–ligand interactions between cells and the surrounding (Fig. 7).[131] Hence, the 3D scaffold environment can influence cell proliferation or direct cell differentiation. Ma *et al.* fabricated 3D polyethylene terephthalate (PET) nonwoven fibrous matrix and modified the pore size and porosity by using thermal compression.[132] Two types of matrices were studied, namely low porosity (LP) and high porosity (HP). The LP matrices had a porosity of 0.849 and an average pore size of 30 μm, while HP matrices had a porosity of 0.896 and an average pore size of 39 μm. When trophoblast ED_{27} cells were cultured on these matrices, the initial cell proliferation rate in the LP matrix was observed to be higher than those in the HP matrix. In addition, cells cultured in the LP matrix were able to spread across adjacent fibers more easily, which led to higher cell proliferation rate. However, the smaller pore sizes of LP matrices limited the formation of large cell aggregates and reduced cell differentiation. Conversely, cells cultured in HP matrices had a higher degree of cell differentiation and aggregation. Besides the trophoblast cells, Takahashi and Tabata also demonstrated the effect of 3D nonwoven matrix fabricated using PET fibers on the proliferation and osteogenic differentiation of rat mesenchymal stem cells (MSCs).[133] Thinner PET fibers resulted in lower cell attachment and caused MSCs to have spherical morphologies due to their smaller diameters. Matrices with bigger PET fiber diameters (i.e., greater than 12 μm) and higher porosity (i.e., approximately 96.7%) enhanced cell proliferation rate, which might be due to facilitated transport of nutrients and oxygen *in vitro*. Thus cellular behavior can be affected by the material properties (e.g., porosity, pore size, interconnectivity, and diameter of fibres) of these 3D nonwoven matrices fabricated from fibers.

The effect of 3D silk fibroin scaffolds on cell proliferation and migration of human foreskin fibroblast showed that pore sizes of 200 to 250 μm and porosity of approximately 86% enabled better cell proliferation.[134] However, cell proliferation of these scaffolds with smaller pore sizes of 100 to 150 μm can be improved by having higher porosity of approximately 91%. Hence, by altering the pore size, porosity, or both parameters, the cell viability and proliferation can be enhanced.[134–137] Besides affecting the cell proliferation capability, it has been shown that the amount of ECM produced, that is, the amount of glycosaminoglycan (GAG) secretion and the expression of collagen gene markers is also affected by the pore size of scaffolds.[138] The study by Lien *et al.* demonstrated that chondrocytes showed preferential proliferation and ECM production for scaffolds with pore sizes between 250 and 500 μm.[138] This pore size range was observed to be capable of maintaining the phenotype of cells, while pores ranging from 50 to 200 μm resulted in cell dedifferentiation.[138] In another study, synthetic human elastin (SHE) scaffolds with an average porosity of 34.4% and mean pore size of 11 μm enabled infiltration of dermal fibroblasts, while a lower average porosity of 14.5% and mean pore size of 8 μm only promoted cell proliferation across the scaffold surface.[139] The fibroblasts cultured in these SHE scaffolds with higher porosity and larger mean pore sizes also deposited fibronectin and collagen type I over the period of cell

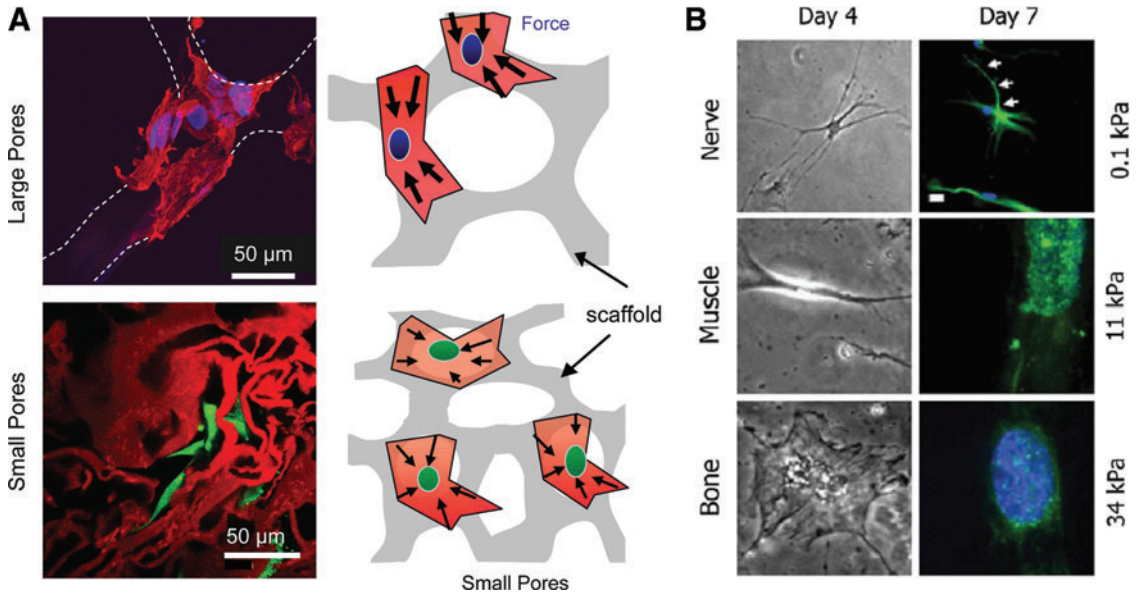

FIG. 7. Effect of **(A)** pore size and **(B)** matrix stiffness on MSC behavior. Actin cyoskeleton and nucleus of MSCs were stained with rhodamine–phalloidin (red) and DAPI (blue). MSCs were observed to be flattened and grow on the wall of the scaffold with large pores (>100 μm). For collagen–glycosaminoglycan scaffold (red) scaffolds with small pores (<50 μm), cells may attach in three-dimensions and differentiate (green nuclei) due to smaller forces present (smaller arrows). When cultured on microenvironments with elasticity of elasticity of 0.1, 11, and 34 kPa, MSCs showed to become neuron-like, myocyte-like, and osteoblasts-like respectively. Images adapted and reproduced by permission of Elsevier.[147] Color images available online at www.liebertpub.com/teb

culture.[139] Thus, the role of porosity and interconnectivity in scaffolds is also to facilitate cell migration within the porous structure such that cell growth is enabled while overcrowding is avoided.

For bone tissue engineering, the optimal pore size for osteoblast activity in tissue engineered scaffolds is still controversial as there have been conflicting reports.[140] In general, scaffolds with pore sizes of about 20 to 1500 μm have been used.[140–143] Akay *et al.* studied the behavior of osteoblasts in PolyHIPE polymer (PHP), a type of highly porous polymeric foam.[144] The osteoblasts were shown to populate more in smaller pores (40 μm) when they were grown in scaffolds with different pore sizes, but larger pore sizes (100 μm) facilitated cell migration. However, the different pore sizes did not have any effect on extent of mineralization or cell penetration depth.[144] Collagen–GAG (CG) scaffolds were also studied to determine its optimal pore size for bone tissue engineering purposes and the effect of pore size on a preosteoblastic cell line, MC3T3-E1.[140] From the results, optimal cell proliferation and infiltration was found in CG scaffolds with mean pore sizes greater than 300 μm. In addition, the ability of larger pores to facilitate cell infiltration was shown to override the beneficial effect of greater initial cell attachment surface areas provided by smaller pores. Hence, this study supported previous reports that suggested the importance of having pore sizes greater than 300 μm for osteogenesis to occur.[145] However, it should be noted that cell differentiation is also dependent on the cell type, scaffold material, and fabrication conditions.[146]

Angiogenesis

Angiogenesis is the growth of new blood vessels from existing vasculature, which is essential to supply oxygen and nutrients to developing tissues, and to facilitate wound healing.[148] Scaffolds were seeded with stem cells and/or endothelial cells or incorporated with angiogenic factors to promote angiogenesis.[148–151] The minimum porosity necessary for the regeneration of a blood vessel is approximately 30 to 40 μm to enable the exchange of metabolic components and to facilitate endothelial cell entrance.[152,153] Artel *et al.* showed that larger pore sizes of approximately 160 to 270 μm facilitated angiogenesis throughout scaffold by using multilayered agent-based model simulation.[154] This model was used to investigate the relationship between angiogenesis and scaffold properties. The materials were assumed to be slowly degrading or nondegradable, such that the pore sizes remained constant. It has also been demonstrated that vascularization of constructs necessitates pores greater than 300 μm.[145,155] The range of pore size suitable for the different types of cellular activities is summarized in Table 1.

Mechanical property

Besides affecting the cell behavior and differentiation potential, the porosity and pore sizes of the scaffolds also have an effect on the mechanical properties. Although higher porosity and pore sizes may facilitate nutrient and oxygen delivery or enable more cell ingrowth, the mechanical properties of the scaffolds will be compromised due to the large amount of void volume.[11] Hence, there is a limit to the amount of porosity or pore sizes that could be incorporated into a scaffold without compromising its mechanical properties to a great extent. In general, scaffolds should have sufficient mechanical strength to maintain integrity until new tissue regeneration. There should also be sufficient space for cells to proliferate and to enable the transport of nutrients and removal of wastes.[20,21] Moreover, it is important that the material property of the scaffolds matches the native tissue *in vivo*, for example, scaffolds fabricated for bone tissue engineering should have comparable strength to the native bone tissue to withstand physiological loadings and to prevent stress shielding from occurring.[20] Although the mechanical property of scaffolds is compromised with higher porosity or pore sizes, the use of materials with high inherent mechanical strength might be a solution to this issue.[134]

Nature's Own Scaffold: The ECM

In native tissues, the ECM is a heterogeneous component of functional proteins, proteoglycans, and signaling molecules arranged in a specific 3D manner enriched with cellular components and a variety of growth factors, cytokines, ions, and water to provide structural support to cells.[171–173] The ECM is an important component in growth and wound healing, and from recent studies it has been shown to be a vital factor in cell signaling.[174–177] Newly formed ECM is secreted by exocytosis after the components are produced by the resident cells. It has now been shown that the ECM is capable of directing cell behavior such as proliferation, differentiation, and migration via biomechanical interactions and mechanical cues.[69] Hence, the ECM is nature's own multifunctional scaffold that not only imparts structural integrity to the tissues, but also modulates a wide range of cellular behaviors.[178] Reviews on the role of ECM properties and mechanism of cell–ECM interactions on cell adhesion, migration, and matrix assembly have been covered by several groups.[179–181]

The ultimate aim of tissue scaffolding strategies is to mimic the actual 3D microenvironment that is the ECM. As with all scaffolds, it is important to consider the pore structure of the native ECM of the tissue that is to be replaced or reconstructed. Different tissues have their own unique ECM composition and structure.[182] In general, the ECM is a porous mesh network of proteins and GAGs that can be altered by cross-linking and enhancing the barrier function of the matrix.[183] Cross-linking of the ECM is associated with local cross-linking of collagen and elastin by lysyl oxidase.[184–186] The increase in cross-linking also inevitably results in a reduction of the matrix porosity. Collagenases can increase the matrix porosity by disrupting the ECM network through uncoiling the triple-helical structure of collagen and exposing sites for proteolysis to occur. ECM degradation, which is associated with matrix metalloproteinases (MMPs), also leads to an increase in porosity.[187,188] Normally, remodeling of the ECM is dependent on the balance between MMPs and tissue inhibitors of metalloproteinases. Remodeling of the ECM is essential to promote normal physiological processes such as development, wound repair, and morphogenesis.[174,187] In fact, changes in ECM structure and composition is also an indication of tissue health and disease progression.[189,190] Some groups have attempted to incorporate biological cues such as MMPs and vascular endothelial growth factor to facilitate ECM degradation, cell proliferation, angiogenesis, or regeneration.[191–193] Amino acid sequence-Arg-Gly-Asp- (RGD)

Table 1. Pore Sizes and Porosity of Various Scaffold Types Required for Different Cellular Activities

Function	*Cell type used/*in vivo *tests*	*Scaffold material*	*Pore size (μm)*	*Porosity (%)*	*Reference*
Angiogenesis	Multilayered agent-based model simulation/*in vivo* rat implantation	Porous PEG	160–270	—	154
Adipogenesis	Murine embryonic stem cells	PCL	6–70	88	156
	Rat BMCs	Silk gland fibroin from nonmulberry	90–110	97	157
	Mice ASCs	Porcine type 1 collagen	70–110	—	158
Cell infiltration	Dermal fibroblasts	Synthetic human elastin	11	34.4	139
	Primary rat osteoblasts	PHP	100	—	144
Chondrogenesis	Human ASCs	PCL	370–400	95	146
	Porcine chondrocytes	Chitosan	70–120	80	159
	Rabbit MSCs	PLGA-GCH	200	74	160
	Rabbit MSCs	PLGA	200–500	—	161
	Porcine chondrocytes	PCL	750	30	162
	Porcine BMSCs	PCL	860	59	162
Hepatogenesis	Human ASCs	PLGA	120–200	—	163
	Rat bone marrow stem cells	c-PLGA	150–350	94	164
Osteogenesis	*In vivo* rat implantation	Hydroxyapatite-BMPs	300–400	—	145
	hMSCs	Coralline hydroxyapatite	200	75	136
	In vivo mice implantation	β-tricalcium phosphate	2–100	75	165
	In vivo mice implantation	Natural coral	150–200	35	166
	RBMSCs	Sintered titanium	250	86	167
	Fetal bovine osteoblasts	PCL	350	65	168
Proliferation	hMSCs	Coralline hydroxyapatite	500	88	136
	Human trophoblast ED27	PET	30	84.9	132
	Rat MSCs	PET	>12	96.7	133
	Human foreskin fibroblasts	Silk fibroin	200–250	86	134
	Human foreskin fibroblasts	Silk fibroin	100–150	91	134
	Rat chondrocytes	Type A gelatin	250–500	—	138
	MC3T3-E1 cells	CG	325	99	140
	Primary rat osteoblasts	PHP	40	—	144
Skin regeneration	Guinea pig dermal and epidermal cells	CG	20–125	—	169
Smooth muscle cell differentitation	Dog BMSCs	PLGA	50–200	—	170

BMCs, bone marrow cells; ASCs, adipose-derived stem cells; hMSCs, human mesenchymal stem cells; BMSCs, bone marrow stem cells; PEG, poly(ethylene glycol); PCL, polycaprolactone; PET, polyethylene terephthalate; CG, Collagen–glycosaminoglycan; PHP, PolyHIPE polymer; cPLGA-GCH, collagen-coated poly-lactide-co-glycolide–gelatin/chondroitin/hyaluronate; BMP, bone morphogenetic protein; RBMSCs, rat bone marrow stromal cells.

peptide can also be attached to scaffolds to enhance cell attachment or mineralization.[194–197]Besides these biological factors, another approach taken to mimic the ECM properties is to directly conjugate ECM molecules to the scaffolds during fabrication or to use decellularized tissues as ECM scaffolds.[198–201] The ECM can be obtained from decellularized tissues and organs, for example, nerve, liver, and respiratory tract.[202–205] The advantage of incorporating ECM into the scaffolds is to improve tissue specificity and to facilitate maintenance of cell functions and phenotype.[205] On the whole, all these different approaches intend to create a 3D microenvironment that behaves like the actual tissue ECM to be successfully used in various tissue engineering applications.

Tunable Scaffolds

Most conventional methods used to fabricate porous scaffolds typically do not allow the porosity or pore size to be tuned once the scaffold is created. In this situation, the use of scaffolds that do not degrade fast enough results in restricted cell migration and proliferation, and nutrient and oxygen deficiencies within the developing tissue. On the other hand, a scaffold that degrades too fast can compromise mechanical and structural integrity of the implant before the tissue is sufficiently well developed. In both cases, tissue regeneration is inhibited due to a mismatch between the rates of tissue growth and scaffold degeneration. The engineering of a "smart" tunable scaffold system that can accommodate widely different regeneration rates of different tissues due to individual differences in age, dietary intake, healing rates, and lifestyle-related factors is thus highly crucial yet challenging. Such scaffolds with postfabrication tunability are essential so as to provide a suitable microenvironment for these dynamic changes, for example, migration and differentiation.[206,207]

Amongst limited literature, the use of photostimulus seems to be popular for on-demand triggered functionalities and tunability in scaffolds. Works reported by Kloxin *et al.* have demonstrated the synthesis of photodegradable macromers and their subsequent polymerization to form hydrogels whose physical, chemical, and biological properties

can be tuned *in situ* and in the presence of cells by ultraviolet, visible, or two-photon irradiation.[208,209] These macromers are cytocompatible and allows remote manipulation of gel properties *in situ*. Postgelation control of the gel properties was demonstrated to introduce temporal changes, creation of arbitrarily shaped features, and on-demand pendant functionality release, which allows cell migration and chondrogenic differentiation of encapsulated stem cells *in vitro*. These photodegradable gels can be used for culturing cells in three dimensions and allowing real-time, externally triggered manipulation of the cell microenvironment to examine its dynamic effect on cell function. However, one disadvantage of this system is the longer degradation time with 365 nm light that may affect cell viability.[208,210]

Various studies on reversible hydrogel fabrication by dimerization of nitrocinnamate have also been tested, but the disadvantage of this system is the requirement of irradiation light in the cytotoxic range (254 nm).[211,212] In another attempt to improve this system, Griffin and Kasko incorporated the photodegradable o-NB linker to various PEG-based macromers such that they can photolyze over a broad range of rates.[212] These hydrogels have been used to encapsulate human MSCs (hMSCs) and the biased release of one stem cell population (green-fluoroescent protein expressing hMSCs) over another (red-fluorescent protein expressing hMSCs) by exploiting the differences in reactivity of two different o-NB linkers was demonstrated.

Conclusion

Porous 3D scaffolds are commonly used in tissue engineering applications and can be fabricated from various conventional and rapid prototyping techniques, depending on the type of materials used or type of pore structures needed. These scaffolds serve to provide suitable microenvironments to support cell growth and function. The structural properties of the scaffolds, for example, porosity and pore size have direct implications on their functionality both *in vitro* and *in vivo*. Generally, interconnected porous scaffold networks that enable the transport of nutrients, removal of wastes, and facilitate proliferation and migration of cells are essential. The porosity and pore size influences cell behavior and determine the final mechanical property of the scaffold. Various techniques, equipments, or computer software have also been developed and used for pore size and porosity measurements.

The purpose of fabricating scaffolds is to produce tissue-like materials such that they can eventually perform like the native tissues. Currently, the idea of scaffold fabrication is based on creating materials with optimum pore size, structure, and porosity for various applications. Generally, scaffolds are first created and cells are subsequently cultured on these scaffolds. As such, there are some existing limitations to this current approach. These prefabricated scaffolds have certain material property that may or may not be suitable to support normal cell growth or differentiation. Incompatibility of the scaffold with the cellular application will eventually lead to the failure of the entire tissue-engineered scaffolding system. Hence, an in-depth analysis is necessary to evaluate the exact porosity and pore size that is optimal for each scaffold system such that they complement the intended type of tissue engineering application. Also, to mimic the actual situation where the ECM undergoes continuous remodeling or healing processes, scaffolds with postfabrication tunability are essential so as to provide a suitable microenvironment for these dynamic changes.

This review provides a general overview that facilitates the understanding of porous scaffold fabrication and pore size and porosity measurement techniques. In addition, the effect of porosity and pore size on cellular behavior and mechanical property of scaffolds was also covered to illustrate the whole concept of the importance of the role of porosity and pore size in tissue engineering applications.

Disclosure Statement

No competing financial interests exist.

References

1. Luu, Y.K., Kim, K., Hsiao, B.S., Chu, B., and Hadjiargyrou, M. Development of a nanostructured DNA delivery scaffold via electrospinning of PLGA and PLA-PEG block copolymers. J Control Release **89,** 341, 2003.
2. Cabral, J., and Moratti, S.C. Hydrogels for biomedical applications. Future Med Chem **3,** 1877, 2011.
3. Eiselt, P., Yeh, J., Latvala, R.K., Shea, L.D., and Mooney, D.J. Porous carriers for biomedical applications based on alginate hydrogels. Biomaterials **21,** 1921, 2000.
4. Kaigler, D., Wang, Z., Horger, K., Mooney, D.J., and Krebsbach, P.H. VEGF scaffolds enhance angiogenesis and bone regeneration in irradiated osseous defects. J Bone Miner Res **21,** 735, 2006.
5. Chiu, Y.C., Larson, J.C., Isom, A., and Brey, E.M. Generation of porous poly(ethylene glycol) hydrogels by salt leaching. Tissue Eng Part C Methods **16,** 905, 2010.
6. Salerno, A., Di Maio, E., Iannace, S., and Netti, P. Tailoring the pore structure of PCL scaffolds for tissue engineering prepared via gas foaming of multi-phase blends. J Porous Mater **19,** 181, 2012.
7. Hollister, S. Porous scaffold design for tissue engineering. Nat Mater **4,** 518, 2005.
8. Liu Tsang, V., and Bhatia, S.N. Three-dimensional tissue fabrication. Adv Drug Deliv Rev **56,** 1635, 2004.
9. Chevalier, E., Chulia, D., Pouget, C., and Viana, M. Fabrication of porous substrates: a review of processes using pore forming agents in the biomaterial field. J Pharm Sci **97,** 1135, 2008.
10. Causa, F., Netti, P.A., and Ambrosio, L. A multi-functional scaffold for tissue regeneration: the need to engineer a tissue analogue. Biomaterials **28,** 5093, 2007.
11. Karageorgiou, V., and Kaplan, D. Porosity of 3D biomaterial scaffolds and osteogenesis. Biomaterials **26,** 5474, 2005.
12. Sung, H.J., Meredith, C., Johnson, C., and Galis, Z.S. The effect of scaffold degradation rate on three-dimensional cell growth and angiogenesis. Biomaterials **25,** 5735, 2004.
13. Buckley, C., and O'Kelly, K. Regular scaffold fabrication techniques for investigations in tissue engineering. In: Prendergast, P.J., and McHugh, P.E., eds. Topics in biomechanical engineering. Dublin, Ireland: Trinity Centre for Bioengineering & National Centre for Biomedical Engineering Science, 2004, pp. 147–166.
14. Ma, P.X. Scaffolds for tissue fabrication. Mater Today **7,** 30, 2004.

15. Pompe, W., Worch, H., Epple, M., Friess, W., Gelinsky, M., Greil, P., Hempel, U., Scharnweber, D., and Schulte, K. Functionally graded materials for biomedical applications. Mater Sci Eng A **362,** 40, 2003.
16. Yeong, W.Y., Chua, C.K., Leong, K.F., and Chandrasekaran, M. Rapid prototyping in tissue engineering: challenges and potential. Trends Biotechnol **22,** 643, 2004.
17. Goulet, R.W., Goldstein, S.A., Ciarelli, M.J., Kuhn, J.L., Brown, M.B., and Feldkamp, L.A. The relationship between the structural and orthogonal compressive properties of trabecular bone. J Biomech **27,** 375, 1994.
18. Chu, T.M.G., Orton, D.G., Hollister, S.J., Feinberg, S.E., and Halloran, J.W. Mechanical and *in vivo* performance of hydroxyapatite implants with controlled architectures. Biomaterials **23,** 1283, 2002.
19. Sherwood, J.K., Riley, S.L., Palazzolo, R., Brown, S.C., Monkhouse, D.C., Coates, M., Griffith, L.G., Landeen, L.K., and Ratcliffe, A. A three-dimensional osteochondral composite scaffold for articular cartilage repair. Biomaterials **23,** 4739, 2002.
20. Leong, K.F., Chua, C.K., Sudarmadji, N., and Yeong, W.Y. Engineering functionally graded tissue engineering scaffolds. J Mech Behav Biomed Mater **1,** 140, 2008.
21. Leong, K.F., Cheah, C.M., and Chua, C.K. Solid freeform fabrication of three-dimensional scaffolds for engineering replacement tissues and organs. Biomaterials **24,** 2363, 2003.
22. Yang, S., Leong, K.F., Du, Z., and Chua, C.K. The design of scaffolds for use in tissue engineering. Part II. Rapid prototyping techniques. Tissue Eng **8,** 1, 2002.
23. Nichol, J.W., and Khademhosseini, A. Modular tissue engineering: engineering biological tissues from the bottom up. Soft Matter **5,** 1312, 2009.
24. Li, C., Vepari, C., Jin, H.J., Kim, H.J., and Kaplan, D.L. Electrospun silk-BMP-2 scaffolds for bone tissue engineering. Biomaterials **27,** 3115, 2006.
25. Zong, X., Bien, H., Chung, C.Y., Yin, L., Fang, D., Hsiao, B.S., Chu, B., and Entcheva, E. Electrospun fine-textured scaffolds for heart tissue constructs. Biomaterials **26,** 5330, 2005.
26. Kim, K., Yu, M., Zong, X., Chiu, J., Fang, D., Seo, Y.S., Hsiao, B.S., Chu, B., and Hadjiargyrou, M. Control of degradation rate and hydrophilicity in electrospun nonwoven poly(D,L-lactide) nanofiber scaffolds for biomedical applications. Biomaterials **24,** 4977, 2003.
27. Chung, H.J., and Park, T.G. Surface engineered and drug releasing pre-fabricated scaffolds for tissue engineering. Adv Drug Deliv Rev **59,** 249, 2007.
28. Lei, B., Shin, K.H., Noh, D.Y., Jo, I.H., Koh, Y.H., Choi, W.Y., and Kim, H.E. Nanofibrous gelatin–silica hybrid scaffolds mimicking the native extracellular matrix (ECM) using thermally induced phase separation. J Mater Chem **22,** 14133, 2012.
29. Montero, R.B., Vial, X., Nguyen, D.T., Farhand, S., Reardon, M., Pham, S.M., Tsechpenakis, G., and Andreopoulos, F.M. bFGF-containing electrospun gelatin scaffolds with controlled nano-architectural features for directed angiogenesis. Acta Biomater **8,** 1778, 2012.
30. Seyednejad, H., Gawlitta, D., Kuiper, R.V., de Bruin, A., van Nostrum, C.F., Vermonden, T., Dhert, W.J.A., and Hennink, W.E. *In vivo* biocompatibility and biodegradation of 3D-printed porous scaffolds based on a hydroxyl-functionalized poly(ε-caprolactone). Biomaterials **33,** 4309, 2012.
31. Seck, T.M., Melchels, F.P.W., Feijen, J., and Grijpma, D.W. Designed biodegradable hydrogel structures prepared by stereolithography using poly(ethylene glycol)/poly(D,L-lactide)-based resins. J Control Release **148,** 34, 2010.
32. Yeong, W.Y., Sudarmadji, N., Yu, H.Y., Chua, C.K., Leong, K.F., Venkatraman, S.S., Boey, Y.C.F., and Tan, L.P. Porous polycaprolactone scaffold for cardiac tissue engineering fabricated by selective laser sintering. Acta Biomater **6,** 2028, 2010.
33. Melchels, F., Wiggenhauser, P.S., Warne, D., Barry, M., Ong, F.R., Chong, W.S., Hutmacher, D.W., and Schantz, J.T. CAD/CAM-assisted breast reconstruction. Biofabrication **3,** 034114, 2011.
34. Duan, B., Wang, M., Zhou, W.Y., Cheung, W.L., Li, Z.Y., and Lu, W.W. Three-dimensional nanocomposite scaffolds fabricated via selective laser sintering for bone tissue engineering. Acta Biomater **6,** 4495, 2010.
35. Elomaa, L., Teixeira, S., Hakala, R., Korhonen, H., Grijpma, D.W., and Seppälä, J.V. Preparation of poly(ε-caprolactone)-based tissue engineering scaffolds by stereolithography. Acta Biomater **7,** 3850, 2011.
36. Ma, P.X., and Langer, R. Fabrication of biodegradable polymer foams for cell transplantation and tissue engineering. Methods Mol Med **18,** 47, 1999.
37. Lu, L., Peter, S.J., Lyman, M.D., Lai, H.L., Leite, S.M., Tamada, J.A., Vacanti, J.P., Langer, R., and Mikos, A.G. *In vitro* degradation of porous poly(L-lactic acid) foams. Biomaterials **21,** 1595, 2000.
38. Lee, S.B., Kim, Y.H., Chong, M.S., Hong, S.H., and Lee, Y.M. Study of gelatin-containing artificial skin V: fabrication of gelatin scaffolds using a salt-leaching method. Biomaterials **26,** 1961, 2005.
39. Chen, G., Ushida, T., and Tateishi, T. Scaffold design for tissue engineering. Macromol Biosci **2,** 67, 2002.
40. Nam, Y.S., Yoon, J.J., and Park, T.G. A novel fabrication method of macroporous biodegradable polymer scaffolds using gas foaming salt as a porogen additive. J Biomed Mater Res **53,** 1, 2000.
41. Mooney, D.J., Baldwin, D.F., Suh, N.P., Vacanti, J.P., and Langer, R. Novel approach to fabricate porous sponges of poly(D,L-lactic-co-glycolic acid) without the use of organic solvents. Biomaterials **17,** 1417, 1996.
42. Keskar, V., Marion, N.W., Mao, J.J., and Gemeinhart, R.A. *In vitro* evaluation of macroporous hydrogels to facilitate stem cell infiltration, growth, and mineralization. Tissue Eng Part A **15,** 1695, 2009.
43. Wachiralarpphaithoon, C., Iwasaki, Y., and Akiyoshi, K. Enzyme-degradable phosphorylcholine porous hydrogels cross-linked with polyphosphoesters for cell matrices. Biomaterials **28,** 984, 2007.
44. Mikos, A., and Temenoff, J. Formation of highly porous biodegradable scaffolds for tissue engineering. Electron J Biotechnol **3,** 23, 2000.
45. Nam, Y.S., and Park, T.G. Porous biodegradable polymeric scaffolds prepared by thermally induced phase separation. J Biomed Mater Res **47,** 8, 1999.
46. Schugens, C., Maquet, V., and Grandfils, C. Biodegradable and macroporous polylactide implants for cell transplantation: 1. Preparation of macroporous polylactide supports by solid-liquid phase separation. Polymer **37,** 1027, 1996.
47. Schugens, C., Maquet, V., Grandfils, C., Jerome, R., and Teyssie, P. Polylactide macroporous biodegradable implants for cell transplantation. II. Preparation of polylactide

foams by liquid-liquid phase separation. J Biomed Mater Res **30,** 449, 1996.
48. Sachlos, E., and Czernuszka, J.T. Making tissue engineering scaffolds work. Review: the application of solid freeform fabrication technology to the production of tissue engineering scaffolds. Eur Cell Mater **5,** 29, 2003.
49. Whang, K., Thomas, C., Healy, K., and Nuber, G. A novel method to fabricate bioabsorbable scaffolds. Polymer **36,** 837, 1995.
50. O'Brien, F.J., Harley, B.A., Yannas, I.V., and Gibson, L. Influence of freezing rate on pore structure in freeze-dried collagen-GAG scaffolds. Biomaterials **25,** 1077, 2004.
51. Wu, C., Luo, Y., Cuniberti, G., Xiao, Y., and Gelinsky, M. Three-dimensional printing of hierarchical and tough mesoporous bioactive glass scaffolds with a controllable pore architecture, excellent mechanical strength and mineralization ability. Acta Biomater **7,** 2644, 2011.
52. Seitz, H., Rieder, W., Irsen, S., Leukers, B., and Tille, C. Three-dimensional printing of porous ceramic scaffolds for bone tissue engineering. J Biomed Mater Res B Appl Biomater **74,** 782, 2005.
53. Curodeau, A., Sachs, E., and Caldarise, S. Design and fabrication of cast orthopedic implants with freeform surface textures from 3-D printed ceramic shell. J Biomed Mater Res **53,** 525, 2000.
54. Kim, S.S., Utsunomiya, H., Koski, J.A., Wu, B.M., Cima, M.J., Sohn, J., Mukai, K., Griffith, L.G., and Vacanti, J.P. Survival and function of hepatocytes on a novel three-dimensional synthetic biodegradable polymer scaffold with an intrinsic network of channels. Ann Surg **228,** 8, 1998.
55. Williams, J.M., Adewunmi, A., Schek, R.M., Flanagan, C.L., Krebsbach, P.H., Feinberg, S.E., Hollister, S.J., and Das, S. Bone tissue engineering using polycaprolactone scaffolds fabricated via selective laser sintering. Biomaterials **26,** 4817, 2005.
56. Hutmacher, D., Sittinger, M., and Risbud, M. Scaffold-based tissue engineering: rationale for computer-aided design and solid free-form fabrication systems. Trends Biotechnol **22,** 354, 2004.
57. Paul, B., and Baskaran, S. Issues in fabricating manufacturing tooling using powder-based additive free-form fabrication. J Mater Proc Technol **61,** 168, 1996.
58. Tan, K.H., Chua, C.K., Leong, K.F., Cheah, C.M., Cheang, P., Abu Bakar, M.S., and Cha, S.W. Scaffold development using selective laser sintering of polyetheretherketone-hydroxyapatite biocomposite blends. Biomaterials **24,** 3115, 2003.
59. Rimell, J.T., and Marquis, P.M. Selective laser sintering of ultra high molecular weight polyethylene for clinical applications. J Biomed Mater Res **53,** 414, 2000.
60. Dhariwala, B., Hunt, E., and Boland, T. Rapid prototyping of tissue-engineering constructs, using photopolymerizable hydrogels and stereolithography. Tissue Eng **10,** 1316, 2004.
61. Draget, K., Skjak-Braek, G., and Smidsrod, O. Alginate based new materials. Int J Biol Macromol **21,** 47, 1997.
62. Wang, W.L., Cheah, C.M., Fuh, J.Y.H., and Lu, L. Influence of process parameters on stereolithography part shrinkage. Materials and Design **17,** 205, 1996.
63. Harris, R., Newlyn, H., Hague, R., and Dickens, P. Part shrinkage anomilies from stereolithography injection mould tooling. Int J Mach Tools Manufacture **43,** 879, 2003.
64. Zein, I., Hutmacher, D.W., Tan, K.C., and Teoh, S.H. Fused deposition modeling of novel scaffold architectures for tissue engineering applications. Biomaterials **23,** 1169, 2002.
65. Xia, Z., Ye, H., Choong, C., Ferguson, D.J.P., Platt, N., Cui, Z., and Triffitt, J.T. Macrophagic response to human mesenchymal stem cell and poly(ε-caprolactone) implantation in nonobese diabetic/severe combined immunodeficient mice. J Biomed Mater Res A **71,** 538, 2004.
66. Choong, C., Triffitt, J., and Cui, Z. Polycaprolactone scaffolds for bone tissue engineering: effects of a calcium phosphate coating layer on osteogenic cells. Food Bioproducts Proc **82,** 117, 2004.
67. Cipitria, A., Skelton, A., Dargaville, T., Dalton, P., and Hutmacher, D. Design, fabrication and characterization of PCL electrospun scaffolds—a review. J Mater Chem **21,** 9419, 2011.
68. Lim, S., and Mao, H. Electrospun scaffolds for stem cell engineering. Adv Drug Deliv Rev **61,** 1084, 2009.
69. Mi, F.L., Shyu, S.S., Chen, C.T., and Schoung, J.Y. Porous chitosan microsphere for controlling the antigen release of Newcastle disease vaccine: preparation of antigen-adsorbed microsphere and *in vitro* release. Biomaterials **20,** 1603, 1999.
70. Pham, Q., Sharma, U., and Mikos, A. Electrospun poly (ε-caprolactone) microfiber and multilayer nanofiber/microfiber scaffolds: characterization of scaffolds and measurement of cellular infiltration. Biomacromolecules **7,** 2796, 2006.
71. Lannutti, J., Reneker, D., Ma, T., Tomasko, D., and Farson, D. Electrospinning for tissue engineering scaffolds. Mater Sci Eng C **27,** 504, 2007.
72. Liang, D., Hsiao, B., and Chu, B. Functional electrospun nanofibrous scaffolds for biomedical applications. Adv Drug Deliv Rev **59,** 1392, 2007.
73. Pramanik, S., Pingguan-Murphy, B., and Osman, N. Progress of key strategies in development of electrospun scaffolds: bone tissue. Sci Technol Adv Mater **13,** 043002, 2012.
74. Lin, S., Bhattacharyya, D., Fakirov, S., Matthews, B., and Cornish, J. Comparison of nanoporous scaffolds manufactured by electrospinning and nanofibrillar composite concept. 18th International Conference on Composite Materials, Edinburgh, Scotland, 2009.
75. Fang, J., Zhang, L., Sutton, D., Wang, X., and Lin, T. Needleless melt-electrospinning of polypropylene nanofibres. J Nanomater **2012,** 16, 2012.
76. Dalton, P.D., Grafahrend, D., Klinkhammer, K., Klee, D., and Möller, M. Electrospinning of polymer melts: phenomenological observations. Polymer **48,** 6823, 2007.
77. Lyons, J., Li, C., and Ko, F. Melt-electrospinning part I: processing parameters and geometric properties. Polymer **45,** 7597, 2004.
78. Ogata, N., Yamaguchi, S., Shimada, N., Lu, G., Iwata, T., Nakane, K., and Ogihara, T. Poly (lactide) nanofibers produced by a melt-electrospinning system with a laser melting device. J Appl Polym Sci **104,** 1640, 2007.
79. Deng, R., Liu, Y., Ding, Y., Xie, P., Luo, L., and Yang, W. Melt electrospinning of low-density polyethylene having a low-melt flow index. J Appl Polym Sci **114,** 166, 2009.
80. Orive, G., Hernández, R.M., Gascón, A.R., Calafiore, R., Chang, T.M.S., De Vos, P., Hortelano, G., Hunkeler, D., Lacík, I., Shapiro, A.M.J., and Pedraz, J.L. Cell encapsulation: promise and progress. Nat Med **9,** 104, 2003.
81. Hu, Y., Grainger, D.W., Winn, S.R., and Hollinger, J.O. Fabrication of poly (α-hydroxy acid) foam scaffolds using multiple solvent systems. J Biomed Mater Res **59,** 563, 2002.

82. Hunt, N., and Grover, L. Cell encapsulation using biopolymer gels for regenerative medicine. Biotechnol Lett **32,** 733, 2010.
83. Nicodemus, G.D., and Bryant, S.J. Cell encapsulation in biodegradable hydrogels for tissue engineering applications. Tissue Eng Part B Rev **14,** 149, 2008.
84. Diaspro, A., Silvano, D., Krol, S., Cavalleri, O., and Gliozzi, A. Single living cell encapsulation in nano-organized polyelectrolyte shells. Langmuir **18,** 5047, 2002.
85. Karoubi, G., Ormiston, M.L., Stewart, D.J., and Courtman, D.W. Single-cell hydrogel encapsulation for enhanced survival of human marrow stromal cells. Biomaterials **30,** 5445, 2009.
86. Uludag, H., De Vos, P., and Tresco, P.A. Technology of mammalian cell encapsulation. Adv Drug Deliv Rev **42,** 29, 2000.
87. de Vos, P., and Marchetti, P. Encapsulation of pancreatic islets for transplantation in diabetes: the untouchable islets. Trends Mol Med **8,** 363, 2002.
88. Loh, Q.L., Wong, Y.Y., and Choong, C. Combinatorial effect of different alginate compositions, polycations, and gelling ions on microcapsule properties. Colloid Polymer Sci **290,** 619, 2012.
89. Acarregui, A., Murua, A., Pedraz, J.L., Orive, G., and Hernández, R.M. A perspective on bioactive cell microencapsulation. BioDrugs **26,** 283, 2012.
90. Städler, B., Price, A.D., and Zelikin, A.N. A critical look at multilayered polymer capsules in biomedicine: drug carriers, artificial organelles, and cell mimics. Adv Funct Mater **21,** 14, 2011.
91. Maspero, F.A., Ruffieux, K., Müller, B., and Wintermantel, E. Resorbable defect analog PLGA scaffolds using CO_2 as solvent: structural characterization. J Biomed Mater Res **62,** 89, 2002.
92. Kim, H.W., Knowles, J.C., and Kim, H.E. Hydroxyapatite/poly(ε-caprolactone) composite coatings on hydroxyapatite porous bone scaffold for drug delivery. Biomaterials **25,** 1279, 2004.
93. Guarino, V., Causa, F., Taddei, P., di Foggia, M., Ciapetti, G., Martini, D., Fagnano, C., Baldini, N., and Ambrosio, L. Polylactic acid fibre-reinforced polycaprolactone scaffolds for bone tissue engineering. Biomaterials **29,** 3662, 2008.
94. Ghasemi-Mobarakeh, L., Semnani, D., and Morshed, M. A novel method for porosity measurement of various surface layers of nanofibers mat using image analysis for tissue engineering applications. J Appl Polym Sci **106,** 2536, 2007.
95. Mayer, R., and Stowe, R. Mercury porosimetry—breakthrough pressure for penetration between packed spheres. J Colloid Sci **20,** 893, 1965.
96. Shum, A.W., Li, J., and Mak, A.F. Fabrication and structural characterization of porous biodegradable poly(dl-lactic-co-glycolic acid) scaffolds with controlled range of pore sizes. Polym Degrad Stability **87,** 487, 2005.
97. Ma, J., Wang, C., and Peng, K. Electrophoretic deposition of porous hydroxyapatite scaffold. Biomaterials **24,** 3505, 2003.
98. Li, W., Laurencin, C., Caterson, E., Tuan, R., and Ko, F. Electrospun nanofibrous structure: a novel scaffold for tissue engineering. J Biomed Mater Res **60,** 613, 2002.
99. Pham, Q., Sharma, U., and Mikos, A. Electrospun poly (ε-caprolactone) microfiber and multilayer nanofiber/microfiber scaffolds: characterization of scaffolds and measurement of cellular infiltration. Biomacromolecules **7,** 2796, 2006.
100. Min, B., Lee, G., Kim, S., Nam, Y., Lee, T., and Park, W. Electrospinning of silk fibroin nanofibers and its effect on the adhesion and spreading of normal human keratinocytes and fibroblasts *in vitro*. Biomaterials **25,** 1289, 2004.
101. y Leon, L., and Carlos, A. New perspectives in mercury porosimetry. Adv Colloid Interface Sci **76,** 341, 1998.
102. Shi, G., Cai, Q., Wang, C., Lu, N., Wang, S., and Bei, J. Fabrication and biocompatibility of cell scaffolds of poly(L-lactic acid) and poly(L-lactic-co-glycolic acid). Polym Adv Technol **13,** 227, 2002.
103. Zhang, Y., and Zhang, M. Synthesis and characterization of macroporous chitosan/calcium phosphate composite scaffolds for tissue engineering. J Biomed Mater Res **55,** 304, 2001.
104. Zhao, F., Yin, Y., Lu, W.W., Leong, J.C., Zhang, W., Zhang, J., Zhang, M., and Yao, K. Preparation and histological evaluation of biomimetic three-dimensional hydroxyapatite/chitosan-gelatin network composite scaffolds. Biomaterials **23,** 3227, 2002.
105. Nazarov, R., Jin, H.J., and Kaplan, D.L. Porous 3-D scaffolds from regenerated silk fibroin. Biomacromolecules **5,** 718, 2004.
106. Zhang, R., and Ma, P.X. Poly(alpha-hydroxyl acids)/hydroxyapatite porous composites for bone-tissue engineering. I. Preparation and morphology. J Biomed Mater Res **44,** 446, 1999.
107. Oh, S.H., Kang, S.G., Kim, E.S., Cho, S.H., and Lee, J.H. Fabrication and characterization of hydrophilic poly(lactic-co-glycolic acid)/poly(vinyl alcohol) blend cell scaffolds by melt-molding particulate-leaching method. Biomaterials **24,** 4011, 2003.
108. Damien, E., Hing, K., Saeed, S., and Revell, P.A. A preliminary study on the enhancement of the osteointegration of a novel synthetic hydroxyapatite scaffold *in vivo*. J Biomed Mater Res A **66,** 241, 2003.
109. El-Ghannam, A.R. Advanced bioceramic composite for bone tissue engineering: design principles and structure-bioactivity relationship. J Biomed Mater Res A **69,** 490, 2004.
110. Kim, H.D., and Valentini, R.F. Retention and activity of BMP-2 in hyaluronic acid-based scaffolds *in vitro*. J Biomed Mater Res **59,** 573, 2002.
111. Park, S.N., Park, J.C., Kim, H.O., Song, M.J., and Suh, H. Characterization of porous collagen/hyaluronic acid scaffold modified by 1-ethyl-3-(3-dimethylaminopropyl)carbodiimide cross-linking. Biomaterials **23,** 1205, 2002.
112. Ho, S.T., and Hutmacher, D.W. A comparison of micro CT with other techniques used in the characterization of scaffolds. Biomaterials **27,** 1362, 2006.
113. Grove, C., and Jerram, D.A. jPOR: an ImageJ macro to quantify total optical porosity from blue-stained thin sections. Comput Geosci **37,** 1850, 2011.
114. Sun, W., Starly, B., Darling, A., and Gomez, C. Computer-aided tissue engineering: application to biomimetic modelling and design of tissue scaffolds. Biotechnol Appl Biochem **39,** 49, 2004.
115. Sun, W., Starly, B., Nam, J., and Darling, A. Bio-CAD modeling and its applications in computer-aided tissue engineering. Comput Aided Des **37,** 1097, 2005.
116. Lee, K., Wang, S., Lu, L., Jabbari, E., Currier, B., and Yaszemski, M. Fabrication and characterization of poly (propylene fumarate) scaffolds with controlled pore structures using 3-dimensional printing and injection molding. Tissue Eng **12,** 2801, 2006.

117. Sell, S., Barnes, C., Simpson, D., and Bowlin, G. Scaffold permeability as a means to determine fiber diameter and pore size of electrospun fibrinogen. J Biomed Mater Res Part A **85,** 115, 2008.
118. Carr, M., and Hardin, C. Fibrin has larger pores when formed in the presence of erythrocytes. Am J Physiol Heart Circ Physiol **253,** H1069, 1987.
119. Carr, M., Shen, L., and Hermans, J. Mass—length ratio of fibrin fibers from gel permeation and light scattering. Biopolymers **16,** 1, 2004.
120. Ghasemi-Mobarakeh, L., Prabhakaran, M., Morshed, M., Nasr-Esfahani, M., and Ramakrishna, S. Electrospun poly (ε-caprolactone)/gelatin nanofibrous scaffolds for nerve tissue engineering. Biomaterials **29,** 4532, 2008.
121. Julve, D., Ramos, J., Pérez, J., and Menéndez, M. Analysis of mercury porosimetry curves of precipitated silica, as an example of compressible porous solids. J Noncrystalline Solids **357,** 1319, 2011.
122. Guldberg, R.E., Duvall, C.L., Peister, A., Oest, M.E., Lin, A.S.P., Palmer, A.W., and Levenston, M.E. 3D imaging of tissue integration with porous biomaterials. Biomaterials **29,** 3757, 2008.
123. Smidsrød, O. Molecular basis for some physical properties of alginates in the gel state. J Chem Soc Faraday Transact **57,** 263, 1974.
124. van Tienen, T.G., Heijkants, R.G.J.C., Buma, P., de Groot, J.H., Pennings, A.J., and Veth, R.P.H. Tissue ingrowth and degradation of two biodegradable porous polymers with different porosities and pore sizes. Biomaterials **23,** 1731, 2002.
125. Bretcanu, O., Samaille, C., and Boccaccini, A.R. Simple methods to fabricate Bioglass®-derived glass–ceramic scaffolds exhibiting porosity gradient. J Mater Sci **43,** 4127, 2008.
126. Harley, B.A., Hastings, A.Z., Yannas, I.V., and Sannino, A. Fabricating tubular scaffolds with a radial pore size gradient by a spinning technique. Biomaterials **27,** 866, 2006.
127. Macchetta, A., Turner, I.G., and Bowen, C.R. Fabrication of HA/TCP scaffolds with a graded and porous structure using a camphene-based freeze-casting method. Acta Biomater **5,** 1319, 2009.
128. Jun, I.K., Koh, Y.H., Song, J.H., Lee, S.H., and Kim, H.E. Improved compressive strength of reticulated porous zirconia using carbon coated polymeric sponge as novel template. Mater Lett **60,** 2507, 2006.
129. Yoon, B.H., Koh, Y.H., Park, C.S., and Kim, H.E. Generation of large pore channels for bone tissue engineering using camphene-based freeze casting. J Am Ceramic Soc **90,** 1744, 2007.
130. Oh, S.H., Park, I.K., Kim, J.M., and Lee, J.H. *In vitro* and *in vivo* characteristics of PCL scaffolds with pore size gradient fabricated by a centrifugation method. Biomaterials **28,** 1664, 2007.
131. Murphy, C., Haugh, M., and O'Brien, F. The effect of mean pore size on cell attachment, proliferation and migration in collagen—glycosaminoglycan scaffolds for bone tissue engineering. Biomaterials **31,** 461, 2010.
132. Ma, T., Li, Y., Yang, S.T., and Kniss, D.A. Effects of pore size in 3-D fibrous matrix on human trophoblast tissue development. Biotechnol Bioeng **70,** 606, 2000.
133. Takahashi, Y., and Tabata, Y. Effect of the fiber diameter and porosity of non-woven PET fabrics on the osteogenic differentiation of mesenchymal stem cells. J Biomater Sci Polym Ed **15,** 41, 2004.
134. Mandal, B., and Kundu, S. Cell proliferation and migration in silk fibroin 3D scaffolds. Biomaterials **30,** 2956, 2009.
135. Kim, U.J., Park, J., Kim, H.J., Wada, M., and Kaplan, D.L. Three-dimensional aqueous-derived biomaterial scaffolds from silk fibroin. Biomaterials **26,** 2775, 2005.
136. Mygind, T., Stiehler, M., Baatrup, A., Li, H., Zou, X., Flyvbjerg, A., Kassem, M., and Bünger, C. Mesenchymal stem cell ingrowth and differentiation on coralline hydroxyapatite scaffolds. Biomaterials **28,** 1036, 2007.
137. Kim, H., Kim, U., Vunjak-Novakovic, G., Min, B., and Kaplan, D. Influence of macroporous protein scaffolds on bone tissue engineering from bone marrow stem cells. Biomaterials **26,** 4442, 2005.
138. Lien, S.M., Ko, L.Y., and Huang, T.J. Effect of pore size on ECM secretion and cell growth in gelatin scaffold for articular cartilage tissue engineering. Acta Biomater **5,** 670, 2009.
139. Rnjak-Kovacina, J., Wise, S., Li, Z., Maitz, P., Young, C., Wang, Y., and Weiss, A. Tailoring the porosity and pore size of electrospun synthetic human elastin scaffolds for dermal tissue engineering. Biomaterials **32,** 6729, 2011.
140. Murphy, C.M., Haugh, M.G., and O'Brien, F.J. The effect of mean pore size on cell attachment, proliferation and migration in collagen-glycosaminoglycan scaffolds for bone tissue engineering. Biomaterials **31,** 461, 2010.
141. Nehrer, S., Breinan, H.A., Ramappa, A., Young, G., Shortkroff, S., Louie, L.K., Sledge, C.B., Yannas, I.V., and Spector, M. Matrix collagen type and pore size influence behaviour of seeded canine chondrocytes. Biomaterials **18,** 769, 1997.
142. Lee, S.J., Lee, I.W., Lee, Y.M., Lee, H.B., and Khang, G. Macroporous biodegradable natural/synthetic hybrid scaffolds as small intestine submucosa impregnated poly(D,L-lactide-co-glycolide) for tissue-engineered bone. J Biomater Sci Polym Ed **15,** 1003, 2004.
143. Baksh, D., Davies, J.E., and Kim, S. Three-dimensional matrices of calcium polyphosphates support bone growth *in vitro* and *in vivo*. J Mater Sci Mater Med **9,** 743, 1998.
144. Akay, G., Birch, M.A., and Bokhari, M.A. Microcellular polyHIPE polymer supports osteoblast growth and bone formation *in vitro*. Biomaterials **25,** 3991, 2004.
145. Kuboki, Y., Jin, Q., and Takita, H. Geometry of carriers controlling phenotypic expression in BMP-induced osteogenesis and chondrogenesis. J Bone Joint Surg Am **83-A Suppl 1,** S105, 2001.
146. Oh, S.H., Kim, T.H., Im, G.I., and Lee, J.H. Investigation of pore size effect on chondrogenic differentiation of adipose stem cells using a pore size gradient scaffold. Biomacromolecules **11,** 1948, 2010.
147. Reilly, G.C., and Engler, A.J. Intrinsic extracellular matrix properties regulate stem cell differentiation. J Biomech **43,** 55, 2010.
148. Sun, H., Wang, X., Hu, X., Yu, W., You, C., Hu, H., and Han, C. Promotion of angiogenesis by sustained release of rhGM-CSF from heparinized collagen/chitosan scaffolds. J Biomed Mater Res B Appl Biomater **100,** 788, 2012.
149. Sun, B., Chen, B., Zhao, Y., Sun, W., Chen, K., Zhang, J., Wei, Z., Xiao, Z., and Dai, J. Crosslinking heparin to collagen scaffolds for the delivery of human platelet-derived growth factor. J Biomed Mater Res B Appl Biomater **91,** 366, 2009.
150. Nillesen, S.T.M., Geutjes, P.J., Wismans, R., Schalkwijk, J., Daamen, W.F., and van Kuppevelt, T.H. Increased angiogenesis and blood vessel maturation in acellular collagen-heparin scaffolds containing both FGF2 and VEGF. Biomaterials **28,** 1123, 2007.

151. Wissink, M.J., Beernink, R., Scharenborg, N.M., Poot, A.A., Engbers, G.H., Beugeling, T., van Aken, W.G., and Feijen, J. Endothelial cell seeding of (heparinized) collagen matrices: effects of bFGF pre-loading on proliferation (after low density seeding) and pro-coagulant factors. J Control Release **67,** 141, 2000.
152. Madden, L.R., Mortisen, D.J., Sussman, E.M., Dupras, S.K., Fugate, J.A., Cuy, J.L., Hauch, K.D., Laflamme, M.A., Murry, C.E., and Ratner, B.D. Proangiogenic scaffolds as functional templates for cardiac tissue engineering. Proc Natl Acad Sci U S A **107,** 15211, 2010.
153. Oliviero, O., Ventre, M., and Netti, P.A. Functional porous hydrogels to study angiogenesis under the effect of controlled release of vascular endothelial growth factor. Acta Biomater **8,** 3294, 2012.
154. Artel, A., Mehdizadeh, H., Chiu, Y.C., Brey, E.M., and Cinar, A. An agent-based model for the investigation of neovascularization within porous scaffolds. Tissue Eng Part A **17,** 2133, 2011.
155. Murphy, C.M., and O'Brien, F.J. Understanding the effect of mean pore size on cell activity in collagen-glycosaminoglycan scaffolds. Cell Adh Migr **4,** 377, 2010.
156. Kang, X., Xie, Y., Powell, H.M., James Lee, L., Belury, M.A., Lannutti, J.J., and Kniss, D.A. Adipogenesis of murine embryonic stem cells in a three-dimensional culture system using electrospun polymer scaffolds. Biomaterials **28,** 450, 2007.
157. Mandal, B.B., and Kundu, S.C. Osteogenic and adipogenic differentiation of rat bone marrow cells on non-mulberry and mulberry silk gland fibroin 3D scaffolds. Biomaterials **30,** 5019, 2009.
158. Itoi, Y., Takatori, M., Hyakusoku, H., and Mizuno, H. Comparison of readily available scaffolds for adipose tissue engineering using adipose-derived stem cells. J Plast ReconstrAesthet Surg **63,** 858, 2010.
159. Griffon, D.J., Sedighi, M.R., Schaeffer, D.V., Eurell, J.A., and Johnson, A.L. Chitosan scaffolds: interconnective pore size and cartilage engineering. Acta Biomater **2,** 313, 2006.
160. Fan, H., Hu, Y., Zhang, C., Li, X., Lv, R., Qin, L., and Zhu, R. Cartilage regeneration using mesenchymal stem cells and a PLGA—gelatin/chondroitin/hyaluronate hybrid scaffold. Biomaterials **27,** 4573, 2006.
161. Uematsu, K., Hattori, K., Ishimoto, Y., Yamauchi, J., Habata, T., Takakura, Y., Ohgushi, H., Fukuchi, T., and Sato, M. Cartilage regeneration using mesenchymal stem cells and a three-dimensional poly-lactic-glycolic acid (PLGA) scaffold. Biomaterials **26,** 4273, 2005.
162. Kemppainen, J.M., and Hollister, S.J. Differential effects of designed scaffold permeability on chondrogenesis by chondrocytes and bone marrow stromal cells. Biomaterials **31,** 279, 2010.
163. Wang, M., Pei, H., Zhang, L., Guan, L., Zhang, R., Jia, Y., Li, B., Yue, W., Wang, Y., and Pei, X. Hepatogenesis of adipose-derived stem cells on poly-lactide-co-glycolide scaffolds: *in vitro* and *in vivo* studies. Tissue Eng Part C Methods **16,** 1041, 2010.
164. Li, J., Tao, R., Wu, W., Cao, H., Xin, J., Guo, J., Jiang, L., Gao, C., Demetriou, A.A., Farkas, D.L., and Li, L. 3D PLGA scaffolds improve differentiation and function of bone marrow mesenchymal stem cell-derived hepatocytes. Stem Cells Dev **19,** 1427, 2010.
165. Kasten, P., Beyen, I., Niemeyer, P., Luginbühl, R., Bohner, M., and Richter, W. Porosity and pore size of beta-tricalcium phosphate scaffold can influence protein production and osteogenic differentiation of human mesenchymal stem cells: an *in vitro* and *in vivo* study. Acta Biomater **4,** 1904, 2008.
166. Chen, F., Mao, T., Tao, K., Chen, S., Ding, G., and Gu, X. Bone graft in the shape of human mandibular condyle reconstruction via seeding marrow-derived osteoblasts into porous coral in a nude mice model. J Oral Maxillofac Surg **60,** 1155, 2002.
167. van den Dolder, J., Farber, E., Spauwen, P.H.M., and Jansen, J.A. Bone tissue reconstruction using titanium fiber mesh combined with rat bone marrow stromal cells. Biomaterials **24,** 1745, 2003.
168. Shor, L., Güçeri, S., Chang, R., Gordon, J., Kang, Q., Hartsock, L., An, Y., and Sun, W. Precision extruding deposition (PED) fabrication of polycaprolactone (PCL) scaffolds for bone tissue engineering. Biofabrication **1,** 015003, 2009.
169. Yannas, I.V., Lee, E., Orgill, D.P., Skrabut, E.M., and Murphy, G.F. Synthesis and characterization of a model extracellular matrix that induces partial regeneration of adult mammalian skin. Proc Natl Acad Sci U S A **86,** 933, 1989.
170. Cho, S.W., Kim, I.K., Lim, S.H., Kim, D.I., Kang, S.W., Kim, S.H., Kim, Y.H., Lee, E.Y., Choi, C.Y., and Kim, B.S. Smooth muscle-like tissues engineered with bone marrow stromal cells. Biomaterials **25,** 2979, 2004.
171. Badylak, S.F. The extracellular matrix as a scaffold for tissue reconstruction. Semin Cell Dev Biol **13**, 377, 2002.
172. Owen, S., and Shoichet, M. Design of three-dimensional biomimetic scaffolds. J Biomed Mater Res Part A **94,** 1321, 2010.
173. Prakash, S., and Chang, T.M. Microencapsulated genetically engineered live *E. coli* DH5 cells administered orally to maintain plasma urea level in uremic rats. Nat Med **2,** 883, 1996.
174. Soon-Shiong, P., Otterlie, M., Skjak-Braek, G., Smidsrod, O., Heintz, R., Lanza, R.P., and Espevik, T. An immunologic basis for the fibrotic reaction to implanted microcapsules. Transplant Proc **23,** 758, 1991.
175. Draget, K.I., and Taylor, C. Chemical, physical and biological properties of alginates and their biomedical implications. Food Hydrocolloids **25,** 251, 2009.
176. Hunkeler, D. Polymers for bioartificial organs. Trends Polym Sci **5,** 286, 1999.
177. Lim, F., and Sun, A.M. Microencapsulated islets as bioartificial endocrine pancreas. Science **210,** 908, 1980.
178. Mørch, Y.A., Donati, I., Strand, B.L., and Skjåk-Braek, G. Effect of Ca^{2+}, Ba^{2+}, and Sr^{2+} on alginate microbeads. Biomacromolecules **7,** 1471, 2006.
179. Leung, A., Nielsen, L., Trau, M., and Timmins, N. Tissue transplantation by stealth—coherent alginate microcapsules for immunoisolation. Biochem Eng J **48,** 337, 2010.
180. Canaple, L., Nurdin, N., Angelova, N., Saugy, D., Hunkeler, D., and Desvergne, B. Maintenance of primary murine hepatocyte functions in multicomponent polymer capsules—in vitro cryopreservation studies. J Hepatol **34,** 11, 2001.
181. Rozario, T., and DeSimone, D. The extracellular matrix in development and morphogenesis: a dynamic view. Dev Biol **341,** 126, 2010.
182. Trivedi, N., Hollister-Lock, J., Lopez-Avalos, M.D., O'Neil, J.J., Keegan, M., Bonner-Weir, S., and Weir, G.C. Increase in beta-cell mass in transplanted porcine neonatal pancreatic cell clusters is due to proliferation of beta-cells and differentiation of duct cells. Endocrinology **142,** 2115, 2001.
183. Ximenes, H.M., Lortz, S., Jörns, A., and Lenzen, S. Triiodothyronine (T3)-mediated toxicity and induction of

apoptosis in insulin-producing INS-1 cells. Life Sci **80,** 2045, 2007.
184. Asfari, M., Janjic, D., Meda, P., Li, G., Halban, P.A., and Wollheim, C.B. Establishment of 2-mercaptoethanol-dependent differentiated insulin-secreting cell lines. Endocrinology **130,** 167, 1992.
185. Bollheimer, L.C., Wrede, C.E., Rockmann, F., Ottinger, I., Schölmerich, J., and Buettner, R. Glucagon production of the rat insulinoma cell line INS-1-A quantitative comparison with primary rat pancreatic islets. Biochem Biophys Res Commun **330,** 327, 2005.
186. Pereverzev, A., Vajna, R., Pfitzer, G., Hescheler, J., Klöckner, U., and Schneider, T. Reduction of insulin secretion in the insulinoma cell line INS-1 by overexpression of a Ca(v)2.3 (alpha1E) calcium channel antisense cassette. Eur J Endocrinol **146,** 881, 2002.
187. MacDonald, M.J., Longacre, M.J., Stoker, S.W., Brown, L.J., Hasan, N.M., and Kendrick, M.A. Acetoacetate and beta-hydroxybutyrate in combination with other metabolites release insulin from INS-1 cells and provide clues about pathways in insulin secretion. Am J Physiol Cell Physiol **294,** C442, 2008.
188. Visse, R., and Nagase, H. Matrix metalloproteinases and tissue inhibitors of metalloproteinases: structure, function, and biochemistry. Circ Res **92,** 827, 2003.
189. Sorokin, L. The impact of the extracellular matrix on inflammation. Nat Rev Immunol **10,** 712, 2010.
190. Pathak, A., and Kumar, S. Independent regulation of tumor cell migration by matrix stiffness and confinement. Proc Natl Acad Sci U S A **109,** 10334, 2012.
191. Rayat, G.R., Rajotte, R.V., and Korbutt, G.S. Potential application of neonatal porcine islets as treatment for type 1 diabetes: a review. Ann N Y Acad Sci **875,** 175, 1999.
192. Kin, T., Korbutt, G.S., Kobayashi, T., Dufour, J.M., and Rajotte, R.V. Reversal of diabetes in pancreatectomized pigs after transplantation of neonatal porcine islets. Diabetes **54,** 1032, 2005.
193. Korbutt, G.S., Elliott, J.F., Ao, Z., Smith, D.K., Warnock, G.L., and Rajotte, R.V. Large scale isolation, growth, and function of porcine neonatal islet cells. J Clin Invest **97,** 2119, 1996.
194. Hohmeier, H.E., and Newgard, C.B. Cell lines derived from pancreatic islets. Mol Cell Endocrinol **228,** 121, 2004.
195. Zimmermann, U., Mimietz, S., Zimmermann, H., Hillgärtner, M., Schneider, H., Ludwig, J., Hasse, C., Haase, A., Rothmund, M., and Fuhr, G. Hydrogel-based non-autologous cell and tissue therapy. Biotechniques **29,** 564, 2000.
196. Thanos, C.G., Bintz, B.E., Bell, W.J., Qian, H., Schneider, P.A., MacArthur, D.H., and Emerich, D.F. Intraperitoneal stability of alginate-polyornithine microcapsules in rats: an FTIR and SEM analysis. Biomaterials **27,** 3570, 2006.
197. Ponce, S., Orive, G., Hernández, R., Gascón, A.R., Pedraz, J.L., de Haan, B.J., Faas, M.M., Mathieu, H.J., and de Vos, P. Chemistry and the biological response against immunoisolating alginate-polycation capsules of different composition. Biomaterials **27,** 4831, 2006.
198. Simpson, N.E., Stabler, C.L., Simpson, C.P., Sambanis, A., and Constantinidis, I. The role of the CaCl2-guluronic acid interaction on alginate encapsulated betaTC3 cells. Biomaterials **25,** 2603, 2004.
199. Constantinidis, I., Grant, S.C., Celper, S., Gauffin-Holmberg, I., Agering, K., Oca-Cossio, J.A., Bui, J.D., Flint, J., Hamaty, C., Simpson, N.E., and Blackband, S.J. Non-invasive evaluation of alginate/poly-l-lysine/alginate microcapsules by magnetic resonance microscopy. Biomaterials **28,** 2438, 2007.
200. Stabler, C., Wilks, K., Sambanis, A., and Constantinidis, I. The effects of alginate composition on encapsulated βTC3 cells. Biomaterials **22,** 1301, 2001.
201. Constantinidis, I., Rask, I., Long, R.C. Jr., and Sambanis, A. Effects of alginate composition on the metabolic, secretory, and growth characteristics of entrapped βTC3 mouse insulinoma cells. Biomaterials **20,** 2019, 1999.
202. Li, H.B., Jiang, H., Wang, C.Y., Duan, C.M., Ye, Y., Su, X.P., Kong, Q.X., Wu, J.F., and Guo, X.M. Comparison of two types of alginate microcapsules on stability and biocompatibility *in vitro* and *in vivo*. Biomed Mater **1,** 42, 2006.
203. Draget, K. I., Smidsrød, O., Skjåk-Bræk, G. Alginates from algae. Biopolymers Online **8,** 215, 2005.
204. Kasimir, M.T., Rieder, E., Seebacher, G., Silberhumer, G., Wolner, E., Weigel, G., and Simon, P. Comparison of different decellularization procedures of porcine heart valves. Int J Artif Organs **26,** 421, 2003.
205. Klokk, T.I., and Melvik, J.E. Controlling the size of alginate gel beads by use of a high electrostatic potential. J Microencapsul **19,** 415, 2002.
206. Kloxin, A., Tibbitt, M., and Anseth, K. Synthesis of photodegradable hydrogels as dynamically tunable cell culture platforms. Nat Protoc **5,** 1867, 2010.
207. Kloxin, A., Tibbitt, M., Kasko, A., Fairbairn, J., and Anseth, K. Tunable hydrogels for external manipulation of cellular microenvironments through controlled photodegradation. Adv Mater **22,** 61, 2009.
208. Kloxin, A., Kasko, A., Salinas, C., and Anseth, K. Photodegradable hydrogels for dynamic tuning of physical and chemical properties. Science **324,** 59, 2009.
209. Forman, J., Dietrich, M., and Monroe, W. Photobiological and thermal effects of photoactivating UVA light doses on cell cultures. Photochem Photobiol Sci **6,** 649, 2007.
210. Andreopoulos, F.M., Deible, C.R., Stauffer, M.T., Weber, S.G., Wagner, W.R., Beckman, E.J., and Russell, A.J. Photoscissable hydrogel synthesis via rapid photopolymerization of novel PEG-based polymers in the absence of photoinitiators. J Am Chem Soc **118,** 6235, 1996.
211. Luo, Y., and Shoichet, M. A photolabile hydrogel for guided three-dimensional cell growth and migration. Nat Mater **3,** 249, 2004.
212. Griffin, D., and Kasko, A. Photodegradable macromers and hydrogels for live cell encapsulation and release. J Am Chem Soc **134,** 13103, 2012.

Address correspondence to:
Cleo Choong, DPhil (Oxon), MBA, MEng (Hons), CEng MIMMM
Division of Materials Technology
School of Materials Science and Engineering
Nanyang Technological University
50 Nanyang Avenue
Singapore 639798
Singapore

E-mail: cleochoong@ntu.edu.sg

Received: July 16, 2012
Accepted: April 23, 2013
Online Publication Date: June 25, 2013